

# On Two Ways of Enumerating Ordered Trees

Italo J. Dejter

University of Puerto Rico

Rio Piedras, PR 00936-8377

[italo.dejter@gmail.com](mailto:italo.dejter@gmail.com)

## Abstract

The middle-levels graph  $M_k$  ( $0 < k \in \mathbb{Z}$ ) has a dihedral quotient pseudograph  $R_k$  whose vertices are the  $k$ -edge ordered trees  $T$ , each  $T$  encoded as a  $(2k+1)$ -string  $F(T)$  formed via  $\rightarrow$ DFS by: (i) ( $\leftarrow$ BFS-assigned) Kierstead-Trotter lexical colors  $0, \dots, k$  for the descending nodes; (ii) asterisks  $*$  for the  $k$  ascending edges. Two ways of corresponding a restricted-growth  $k$ -string  $\alpha$  to each  $T$  exist, namely one Stanley's way and a novel way that assigns  $F(T)$  to  $\alpha$  via nested substring-swaps. These swaps permit to sort  $V(R_k)$  as an ordered tree that allows a lexical visualization of  $M_k$  as well as the Hamilton cycles of  $M_k$  constructed by P. Gregor, T. Mütze and J. Nummenpalo.

## 1 Introduction

Let  $0 < k \in \mathbb{Z}$  and let  $n = 2k + 1$ . The *middle-levels graph*  $M_k$  [3] is the subgraph of the Hasse diagram [8] of the Boolean lattice  $2^{[n]}$  induced by its  $k$ - and  $(k+1)$ -th levels (i.e. formed by the  $k$ - and  $(k+1)$ -subsets of  $[n] = \{0, \dots, 2k\}$ ). The dihedral group  $D_{2n}$  acts on  $M_k$  via translations mod  $n$  (see Section 4) and complemented reversals (see Section 5).

Let  $C_k = \frac{(2k)!}{k!(k+1)!}$  be the  $k$ -th Catalan number [9] [A000108](#). Let  $\mathcal{S}$  be the sequence [9] [A239903](#) of *restricted-growth strings* or *RGS's* ([1] page 325). We will show that the first  $C_k$  terms of  $\mathcal{S}$  stand for the orbits of  $V(M_k)$  under the natural  $D_{2n}$ -action on  $(V(M_k), E(M_k))$  in two ways: as Stanley's  $k$ -*RGS's* (see below) and as  $k$ -*germs*, proposed in this work.

In Section 6, the mentioned  $D_{2n}$ -action will allow to project  $M_k$  onto a quotient pseudograph  $R_k$  whose vertices stand for the first  $C_k$  terms of  $\mathcal{S}$  via the Kierstead-Trotter lexical-matching [3] color (or *lexical color*) set  $[k+1] = \{0, 1, \dots, k\}$  on the  $k+1$  edges incident to each vertex (Sections 7, 8 and 14).

In preparation, RGS's are first tailored in Section 2 into numerical  $(k-1)$ -strings  $\alpha$  that are our  $k$ -*germs*. These yield  $n$ -strings  $F(\alpha)$  (Section 3), each composed by the  $k+1$  lexical colors, as well as by  $k$  asterisks  $*$ . The  $F(\alpha)$ 's represent the  $k$ -edge ordered trees (Proposition 1) and are obtained via a nested substring-swapping, here called *castling* (Theorem 3), that sorts them linearly via pruning and regrafting. These trees (encoded as  $F(\alpha)$ ) represent the vertices of  $R_k$  via a corresponding *uncastling* procedure (Section 8).

The mentioned linear sorting arises from an ordered tree  $\mathcal{T}_k$  (Theorem 2) with  $|V(\mathcal{T}_k)| = |V(R_k)| = C_k$ . This  $\mathcal{T}_k$  controls  $V(R_k)$  and allows to lexically visualize  $V(M_k)$ . On the other hand, an all-RGS's binary tree is given in Section 9, representing the vertices (i.e. the ordered trees) of all  $R_k$ 's. This is a unifying pattern for the presentation of all the  $V(M_k)$ 's.

It is known that the  $k$ -edge ordered trees (that is, the vertices of  $R_k$ ) denoted by R. Stanley in [10] page 221 item (e) as “plane trees with  $k+1$  vertices”, are equivalent to  $k$ -strings with initial entry 0, that we shall call  $k$ -*RGS's*, tailored from RGS's in a different way

([10] page 224 item (u)) from that of our *k-germs*. An equivalence of *k-germs* and *k-RGS's* is presented in Section 10 via their distinct relation to the *k-edge ordered trees*.

Our approach yields a stepwise-reversing presentation (i.e., via complemented-reversal adjacency) of the Hamilton cycles of  $M_k$  [4, 5, 6, 7] in P. Gregor, T. Mütze and J. Nummenpalo [2], that allows an explicit view of all Kierstead-Trotter lexical colors in ordered trees  $F(\alpha)$ . In fact, the 2-factor  $W_{01}^k$  of  $R_k$  determined by the colors 0 and 1 is first reanalyzed from this viewpoint in Section 11. Then,  $W_{01}^k$  is seen in Section 12 to morph into such Hamilton cycles via symmetric differences with 6-cycles having a simpler form this way.

Moreover, an integer sequence  $\mathcal{S}_0$  is shown to exist such that, for each  $k > 0$ , the neighbors of the vertices of  $R_k$  via color- $k$  edges have their RGS's ordered as in  $\mathcal{S}$  corresponding to an idempotent permutation on the first  $C_k$  terms of  $\mathcal{S}_0$ . This and related properties hold for lexical colors  $0, 1, \dots, k$  (Theorem 15 and Remarks 16-18) reflecting properties of plane trees (i.e., classes of ordered trees under root rotation) from Observation 11 in Section 11.

Furthermore, Section 13 considers the pertaining symmetry properties obtained by reversing the designation of the roots in the ordered trees so that each color- $i$  adjacency ( $0 \leq i \leq k$ ) can be seen from the lexical-color  $(k - i)$  viewpoint. In addition, Section 15, presents an alternate way to  $R_k$ .

## 2 From Restricted-Growth Strings to *k*-Germs

Let  $0 < k \in \mathbb{Z}$ . We can express the mentioned sequence  $\mathcal{S}$  as:  $\mathcal{S} = (\beta(0), \dots, \beta(17), \dots) =$

$$(0, 1, 10, 11, 12, 100, 101, 110, 111, 112, 120, 121, 122, 123, 1000, 1001, 1010, 1011, \dots) \quad (1)$$

and note that  $\mathcal{S}$  has the lengths of its contiguous pairs  $(\beta(i-1), \beta(i))$  constant unless  $i = C_k$  for  $0 < k \in \mathbb{Z}$ , in which case  $\beta(i-1) = \beta(C_k-1) = 12 \cdots k$  and  $\beta(i) = \beta(C_k) = 10^k = 10 \cdots 0$ .

To view the continuation of  $\mathcal{S}$ , each RGS  $\beta = \beta(m)$  is transformed, for every  $k \in \mathbb{Z}$  with  $k \geq \text{length}(\beta)$ , into a  $(k-1)$ -string  $\alpha = a_{k-1}a_{k-2} \cdots a_2a_1$  by prefixing  $k - \text{length}(\beta)$  zeros to  $\beta$ . As hinted in Section 1, we say that such an  $\alpha$  is a *k-germ*. In fact, a *k-germ*  $\alpha$  ( $1 < k \in \mathbb{Z}$ ) is a  $(k-1)$ -string  $\alpha = a_{k-1}a_{k-2} \cdots a_2a_1$  such that:

- (1) the leftmost position (called position  $k-1$ ) of  $\alpha$  contains entry  $a_{k-1} \in \{0, 1\}$ ;
- (2) given  $1 < i < k$ , the entry  $a_{i-1}$  (at position  $i-1$ ) satisfies  $0 \leq a_{i-1} \leq a_i + 1$ .

Every *k-germ*  $a_{k-1}a_{k-2} \cdots a_2a_1$  yields the  $(k+1)$ -germ  $0a_{k-1}a_{k-2} \cdots a_2a_1$ . A *non-null* RGS is obtained by stripping a *k-germ*  $\alpha = a_{k-1}a_{k-2} \cdots a_1 \neq 00 \cdots 0$  off all the null entries to the left of its leftmost position containing a 1. We denote such an RGS again by  $\alpha$ , convene that the *null* RGS  $\alpha = 0$  is stripped from all null *k-germs*  $\alpha$  ( $0 < k \in \mathbb{Z}$ ), and use notation  $\alpha = \alpha(m)$  (or  $\beta = \beta(m)$ , as in (1)) both for a *k-germ* and for its corresponding RGS.

The *k-germs* are ordered as follows. Given two *k-germs*, say  $\alpha = a_{k-1} \cdots a_2a_1$  and  $\beta = b_{k-1} \cdots b_2b_1$ , where  $\alpha \neq \beta$ , we say that  $\alpha$  precedes  $\beta$ , written  $\alpha < \beta$ , whenever either:

- (i)  $a_{k-1} < b_{k-1}$  or
- (ii)  $a_j = b_j$ , for  $k-1 \leq j \leq i+1$ , and  $a_i < b_i$ , for some  $k-1 > i \geq 1$ .

The resulting order on  $k$ -germs  $\alpha(m)$ ,  $(m \leq C_k)$ , corresponding biunivocally (via the assignment  $m \rightarrow \alpha(m)$ ) with the natural order on  $m$ , yields a listing that we call the *natural* ( $k$ -germ) *listing*. Note that there are exactly  $C_k$   $k$ -germs  $\alpha = \alpha(m) < 10^k$ ,  $\forall k > 0$ . Section 16, deals with the determination of these RGS's and  $k$ -germs.

### 3 Nested Substring-Swaps in $n$ -Strings

An *ordered* (rooted) *tree* [2] is a tree  $T$  with: **(a)** a node  $v_0$  as its root; **(b)** an embedding of  $T$  into the plane with  $v_0$  on top; **(c)** the edges between the nodes at distances  $j$  and  $j + 1$  from  $v_0$  ( $0 \leq j < \text{height}(T)$ ) having parent nodes at the  $j$ -level above their children at the  $(j + 1)$ -level; **(d)** the children in (c) ordered from left to right.

TABLE I

$m$	$\alpha$	$\beta$	$F(\beta)$	$i$	$W^i   X   Y   Z^i$	$W^i   Y   X   Z^i$	$F(\alpha)$	$\alpha$
0	0	—	—	—	—	—	012**	0
1	1	0	012**	1	0 1 2* *	0 2* 1 *	02*1*	1
0	00	—	—	—	—	—	0123***	00
1	01	00	0123***	1	0 1 23** *	0 23** 1 *	023**1*	01
2	10	00	0123***	2	01 2 3* **	01 3* 2 **	013*2**	10
3	11	10	013*2**	1	0 13* 2* *	0 2* 13* *	02*13**	11
4	12	11	02*13**	1	0 2*1 3* *	0 3* 2*3 *	03*2*1*	12
0	000	—	—	—	—	—	01234****	000
1	001	000	01234****	1	0 1 234**** *	0 234**** 1 *	0234****1*	001
2	010	000	01234****	2	01 2 34**** *	01 34**** 2 *	0134****2*	010
3	011	010	0134**2**	1	0 134** 2* *	0 2* 134** *	02*134***	011
4	012	011	02*134***	1	0 2*1 34*** *	0 34*** 2*1 *	034***2*1*	012
5	100	000	01234***	3	012 3 4* ***	012 4* 3 ***	0124*3***	100
6	101	100	0124*3***	1	0 1 24* 3** *	0 24* 3** 1 *	024*3***1*	101
7	110	100	0124*3***	2	01 24* 3** *	01 3* 24* **	013*24***	110
8	111	110	013*24***	1	0 13* 24** *	0 24** 13* *	024**13**	111
9	112	111	024**13**	1	0 24** 13* *	0 3* 24** 1 *	03*24**1*	112
10	120	110	013*24***	2	01 3*2 4* **	01 4* 3*2 **	014*3*2**	120
11	121	120	014*3*2**	1	0 14*3* 2* *	0 2* 14*3* *	02*14*3**	121
12	122	121	02*14*3**	1	0 2*34* 3* *	0 3* 2*14* *	03*2*14**	122
13	123	122	03*2*14**	1	0 3*2*1 4* *	0 4* 3*2*1 *	04*3*2*1*	123

**Proposition 1.** *Each  $k$ -edge ordered tree  $T$  is represented biunivocally by an  $n$ -string  $F(T)$ .*

*Proof.* We perform a depth first search ( $\rightarrow$ DFS) on  $T$  with its vertices from  $v_0$  downward denoted  $v_i$  ( $i = 0, 1, \dots, k$ ) in a right-to-left breadth-first search ( $\leftarrow$ BFS) way. Such DFS yields the claimed  $F(\alpha)$  by writing successively from left to right:

(i) the subindex  $i$  of each  $v_i$  in the  $\rightarrow$ DFS downward appearance and

(ii) an asterisk for each edge  $e_i$  with child  $v_i$  in the  $\rightarrow$ DFS upward appearance.  $\square$

**Theorem 2.** Each  $k$ -germ  $\alpha = a_{k-1} \cdots a_1 \neq 0^{k-1}$  with rightmost nonzero entry  $a_i$  ( $1 \leq i = i(\alpha) < k$ ) corresponds to a  $k$ -germ  $\beta(\alpha) = b_{k-1} \cdots b_1 < \alpha$  having  $b_i = a_i - 1$  and  $a_j = b_j$  for  $j \neq i$ . Moreover,  $k$ -germs are the vertices of an ordered tree  $\mathcal{T}_k$  rooted at  $0^{k-1}$ , each  $k$ -germ  $\alpha \neq 0^{k-1}$  having  $\beta(\alpha)$  as its parent so that the edge  $\beta(\alpha)\alpha$  of  $\mathcal{T}_k$  between  $\beta(\alpha)$  and  $\alpha$  admits a label  $i = i(\alpha)$ . Furthermore, the existence of  $\mathcal{T}_k$  allows to sort all  $k$ -germs linearly.

*Proof.* The statement, illustrated for  $k = 2, 3, 4$  in the first three columns of Table I, is straightforward. Table I also serves as illustration for the proof of Theorem 3, below.  $\square$

By representing  $\mathcal{T}_k$  with each node  $\beta$  having its children  $\alpha$  enclosed between parentheses following  $\beta$  and separating siblings with commas, we can write:

$$\mathcal{T}_4 = 000(001, 010(011(012))), 100(101, 110(111(121))), 120(121(122(123)))).$$

**Theorem 3.** To each  $k$ -germ  $\alpha = a_{k-1} \cdots a_1$  corresponds biunivocally an  $n$ -string  $F(\alpha) = F(T) = f_0 f_1 \cdots f_{2k}$  whose entries are  $0, 1, \dots, k$  (once each) and  $k$  asterisks  $*$  such that:

- (A)  $T$  is a  $k$ -edge ordered tree; (B)  $F(0^{k-1}) = 012 \cdots (k-1)k * \cdots *$ ;
- (C) if  $\alpha \neq 0^{k-1}$ , then  $F(\alpha)$  is obtained from  $F(\beta) = F(\beta(\alpha)) = h_0 h_1 \cdots h_{2k}$  as in Theorem 2 via the following Nested String Swapping (Castling) Procedure, where  $i = i(\alpha)$ :

1. let  $W^i = h_0 h_1 \cdots h_{i-1} = f_0 f_1 \cdots f_{i-1}$  and  $Z^i = h_{2k-i+1} \cdots h_{2k-1} h_{2k} = f_{2k-i+1} \cdots f_{2k-1} f_{2k}$  be respectively the initial and terminal substrings of length  $i = i(\alpha)$  in  $F(\beta)$ ;
2. let  $\Omega > 0$  be the leftmost entry of the substring  $U = F(\beta) \setminus (W^i \cup Z^i)$  and consider the concatenation  $U = X|Y$ , with  $Y$  starting at entry  $\Omega + 1$ ; then,  $F(\beta) = W^i|X|Y|Z^i$ ;
3. set  $F(\alpha) = W^i|Y|X|Z^i$ , (the result of swapping the nested substring  $X|Y$ , yielding  $Y|X$ ).

In particular: (a) the leftmost entry,  $f_0$ , of each  $F(\alpha)$  is 0; (b)  $k*$  is a substring of  $F(\alpha)$ ;

- (c) each  $f_j \in [0, k]$  with  $f_{j+1} \in [0, k]$  satisfies  $f_j < f_{j+1}$ , where  $j \in [0, 2k]$ ;
- (d) each substring  $f_j * \cdots * f_{j'}$  of  $F(\alpha)$  ( $j'' \in (j, j') \subset [0, 2k] \Rightarrow f_{j''} = *$ ) has  $f_{j'} < f_j$ ;
- (e)  $W^i$  is an  $i$ -substring with no asterisks; (f)  $Z^i$  is formed exactly by  $i$  asterisks.

*Proof.* Let  $\alpha = a_{k-1} \cdots a_1 \neq 0^{k-1}$  be a  $k$ -germ. In the sequence of (nested substring-swap) applications of steps 1-3 along the path from root  $0^{k-1}$  to  $\alpha$  in  $\mathcal{T}_k$ , unit augmentation of  $a_i$  for larger values of  $i$  ( $0 < i < k$ ) must occur earlier, and then in strictly descending order of the entries  $i$  of the intermediate  $k$ -germs. As a result, the length of the inner substring  $X|Y$  is kept non-decreasing after each application. This is illustrated in Table I, where the order of presentation of  $X$  and  $Y$  is reversed in successively decreasing steps. In the process, items (a)-(e) are seen to be fulfilled.

The three successive subtables in Table I have  $C_k$  rows each, where  $C_2 = 2$ ,  $C_3 = 5$  and  $C_4 = 14$ ; in the subtables, the  $k$ -germs  $\alpha$  are shown both on the second and last columns via natural enumeration in the first column; the images  $F(\alpha)$  of those  $\alpha$  are shown on the penultimate column; the remaining columns in the table are filled, from the second row on, as follows: (i)  $\beta = \beta(\alpha)$ , arising in Theorem 2; (ii)  $F(\beta)$ , taken from the penultimate column in the previous row; (iii) the length  $i$  of  $W^i$  and  $Z^i$  ( $1 \leq i \leq k-1$ ); (iv) the decomposition  $W^i|Y|X|Z^i$  of  $F(\beta)$ ; (v) the nested swapping  $W^i|Y|Z^i$  of  $W^i|Y|X|Z^i$ , re-concatenated in the following, penultimate, column as  $F(\alpha)$ , with  $\alpha = F^{-1}(F(\alpha))$  in the last column.  $\square$

In the context of the results above, let  $T = T_\alpha$ , so  $F(T_\alpha) = F(\alpha)$ . For each  $k$ -germ  $\alpha \neq 0^{k-1}$ , Theorem 3 carries a *tree-surgery transformation* from  $T_\beta$  onto  $T_\alpha$  by *pruning-and-regrafting* of an adequate subtree of  $T_\beta$  via the vertices  $v_i$  and the edges  $e_i$ , with parent vertices reattached in a substring swapping way. Proposition 1 is used in Sections 11-13 in giving a stepwise-reversing view of Hamilton cycles [2] in the  $M_k$ 's. In Section 13, an alternate viewpoint on ordered trees taking  $a_k$  as the root instead of  $a_0$  is considered.

TABLE II

$m$	$\alpha$	$\theta(\alpha)$	$\hat{\theta}(\alpha)$	$\hat{\aleph}(\theta(\alpha)) = \aleph(\hat{\theta}(\alpha))$	$\aleph(\theta(\alpha))$
0	0	00011	$0_00_10_21_11_*$	$0_*0_*1_21_11_0$	00111
1	1	00101	$0_00_21_*0_11_*$	$0_*1_10_*1_21_0$	01011
0	00	0000111	$0_00_10_20_31_11_1*$	$0_*0_*0_*1_31_21_11_0$	0001111
1	01	0001101	$0_00_20_31_11_01_1*$	$0_*1_10_*0_*1_31_21_0$	0100111
2	10	0001011	$0_00_10_32_01_11_1*$	$0_*0_*1_20_*1_31_11_0$	0010111
3	11	0010011	$0_00_21_*0_10_31_11_*$	$0_*0_*1_31_10_*1_21_0$	0011011
4	12	0010101	$0_00_31_*0_21_*0_11_*$	$0_*1_10_*1_20_*1_31_0$	0101011

Each  $F(\alpha)$  corresponds to a binary  $n$ -string  $\theta(\alpha)$  of weight  $k$  obtained by replacing each number in  $[k+1]$  by 0 and each asterisk  $*$  by 1. By attaching the entries of  $F(\alpha)$  as subscripts to the corresponding entries of  $\theta(\alpha)$ , a subscripted binary  $n$ -string  $\hat{\theta}(\alpha)$  is obtained, as shown for  $k = 2, 3$  in the fourth column of Table II. Let  $\aleph(\theta(\alpha))$  be given by the *complemented reversal* of  $\theta(\alpha)$ , that is:

$$\text{if } \theta(\alpha) = a_0a_1 \cdots a_{2k}, \text{ then } \aleph(\theta(\alpha)) = \bar{a}_{2k} \cdots \bar{a}_1 \bar{a}_0, \quad (2)$$

where  $\bar{0} = 1$  and  $\bar{1} = 0$ . A subscripted version  $\hat{\aleph}$  of  $\aleph$  is obtained for  $\hat{\theta}(\alpha)$ , as shown in the fifth column of Table II, with the subscripts of  $\hat{\aleph}$  reversed with respect to those of  $\aleph$ . Each image of a  $k$ -germ  $\alpha$  under  $\aleph$  is an  $n$ -string of weight  $k+1$  and has the 1's indexed with subscripts in  $[k+1]$  and the 0's indexed with asterisk subscript. The subscripts in  $[k+1]$  reappear from Section 7 on as lexical colors for the graphs  $M_k$ .

## 4 Translations mod $n$ in $M_k$

The *n-cube graph*  $H_n$  is the Hasse diagram of the Boolean lattice  $2^{[n]}$  on the set  $[n]$ . We will express each vertex  $v$  of  $H_n$  in three equivalent ways, namely, as:

- (a) ordered set  $A = \{a_0, a_1, \dots, a_{j-1}\} = a_0a_1 \cdots a_{j-1} \subseteq [n]$  that  $v$  represents,  $(0 < j \leq n)$ ;
- (b) characteristic binary  $n$ -vector  $B_A = (b_0, b_1, \dots, b_{n-1})$  of ordered set  $A$  in (a) above, where  $b_i = 1$  if and only if  $i \in A$ ,  $(i \in [n])$ ;
- (c) polynomial  $\epsilon_A(x) = b_0 + b_1x + \cdots + b_{n-1}x^{n-1}$  associated to  $B_A$  in (b) above.

The ordered set  $A$  and the vector  $B_A$  in (a) and (b) respectively are written for short as  $a_0a_1 \cdots a_{j-1}$  and  $b_0b_1 \cdots b_{n-1}$ .  $A$  is said to be the *support* of  $B_A$ .

For each  $j \in [n]$ , let  $L_j = \{A \subseteq [n]; |A| = j\}$  be the  $j$ -level of  $H_n$ . Then,  $M_k$  is the subgraph of  $H_n$  induced by  $L_k \cup L_{k+1}$ , for  $1 \leq k \in \mathbb{Z}$ . By viewing the elements of  $V(M_k) = L_k \cup L_{k+1}$  as polynomials, as in (c) above, a regular (i.e., free and transitive) translation mod  $n$  action  $\Upsilon'$  of  $\mathbb{Z}_n$  on  $V(M_k)$  is seen to exist, given by:

$$\Upsilon' : \mathbb{Z}_n \times V(M_k) \rightarrow V(M_k), \text{ with } \Upsilon'(i, v) = v(x)x^i \pmod{1+x^n}, \quad (3)$$

where  $v \in V(M_k)$  and  $i \in \mathbb{Z}_n$ . Now,  $\Upsilon'$  yields a quotient graph  $M_k/\pi$  of  $M_k$ , where  $\pi$  stands for the equivalence relation on  $V(M_k)$  given by:

$$\epsilon_A(x)\pi\epsilon_{A'}(x) \iff \exists i \in \mathbb{Z} \text{ with } \epsilon_{A'}(x) \equiv x^i\epsilon_A(x) \pmod{1+x^n},$$

with  $A, A' \in V(M_k)$ . This is to be used in the proofs of Theorems 5 and 13. Clearly,  $M_k/\pi$  is the graph whose vertices are the equivalence classes of  $V(M_k)$  under  $\pi$ . Notice that  $\pi$  induces a partition of  $E(M_k)$  into equivalence classes that are the edges of  $M_k/\pi$ .

## 5 Complemented Reversals in $M_K$

Let  $(b_0b_1 \cdots b_{n-1})$  denote the class of  $b_0b_1 \cdots b_{n-1} \in L_i$  in  $L_i/\pi$ . Let  $\rho_i : L_i \rightarrow L_i/\pi$  be the canonical projection given by  $\rho(b_0b_1 \cdots b_{n-1}) = (b_0b_1 \cdots b_{n-1})$ , for  $i \in \{k, k+1\}$ . The definition of the complemented reversal  $\aleph$  in display (2) is easily extended to a bijection, again denoted  $\aleph$ , from  $L_k$  onto  $L_{k+1}$ . Let  $\aleph_\pi : L_k/\pi \rightarrow L_{k+1}/\pi$  be given by  $\aleph_\pi((b_0b_1 \cdots b_{n-1})) = (\bar{b}_{n-1} \cdots \bar{b}_1 \bar{b}_0)$ . Note  $\aleph_\pi$  is a bijection and the identities  $\rho_{k+1}\aleph = \aleph_\pi\rho_k$  and  $\rho_k\aleph^{-1} = \aleph_\pi^{-1}\rho_{k+1}$ .

The following geometric representations are handy. List vertically the vertex parts  $L_k$  and  $L_{k+1}$  of  $M_k$  (resp.  $L_k/\pi$  and  $L_{k+1}/\pi$  of  $M_k/\pi$ ) so as to display a splitting of  $V(M_k) = L_k \cup L_{k+1}$  (resp.  $V(M_k)/\pi = L_k/\pi \cup L_{k+1}/\pi$ ) into pairs, each pair contained in a horizontal line, the two composing vertices of such pair equidistant from a vertical line  $\phi$  (resp.  $\phi/\pi$ , depicted through  $M_2/\pi$  on the left of Figure 1, Section 6 below). In addition, we impose that each resulting horizontal vertex pair in  $M_k$  (resp.  $M_k/\pi$ ) be of the form  $(B_A, \aleph(B_A))$  (resp.  $((B_A), (\aleph(B_A))) = \aleph_\pi((B_A))$ ), disposed from left to right at both sides of  $\phi$ . In this context, a non-horizontal edge of  $M_k/\pi$  is said to be a *skew edge*.

**Theorem 4.** *Each skew edge  $e = (B_A)(B_{A'})$  of  $M_k/\pi$  corresponds to another skew edge  $\aleph_\pi((B_A))\aleph_\pi^{-1}((B_{A'}))$  obtained from  $e$  by reflection on the line  $\phi/\pi$ . Moreover:*

- (i) *the skew edges of  $M_k/\pi$  appear in pairs, with the endpoints of the edges in each pair forming two horizontal pairs of vertices equidistant from  $\phi/\pi$ ;*
- (ii) *each horizontal edge of  $M_k/\pi$  has multiplicity equal either to 1 or to 2.*

*Proof.* The skew edges  $B_A B_{A'}$  and  $\aleph^{-1}(B_{A'})\aleph(B_A)$  of  $M_k$  are reflection of each other about  $\phi$ . Their endpoints form two horizontal pairs  $(B_A, \aleph(B_{A'}))$  and  $(\aleph^{-1}(B_A), B_{A'})$  of vertices. Now,  $\rho_k$  and  $\rho_{k+1}$  extend together to a covering graph map  $\rho : M_k \rightarrow M_k/\pi$ , since the edges accompany the projections correspondingly, exemplified for  $k = 2$  as follows:

$$\begin{aligned} \aleph((B_A)) &= \aleph((00011)) = \aleph(\{00011, 10001, 11000, 01100, 00110\}) = \{00111, 01110, 11100, 11001, 10011\} = (00111), \\ \aleph^{-1}((B'_A)) &= \aleph^{-1}((01011)) = \aleph^{-1}(\{01011, 10110, 10110, 11010, 10101\}) = \{00101, 10010, 01001, 10100, 01010\} = (00101). \end{aligned}$$

Here, the order of the elements in the image of class (00011) (resp. (01011)) mod  $\pi$  under  $\aleph$  (resp.  $\aleph^{-1}$ ) are shown reversed, from right to left (cyclically between braces, continuing on the right once one reaches the leftmost brace). Such reversal holds for every  $k > 2$ :

$$\begin{aligned} \aleph((B_A)) &= \aleph((b_0 \cdots b_{2k})) = \aleph(\{b_0 \cdots b_{2k}, b_{2k} \cdots b_{2k-1}, \dots, b_1 \cdots b_0\}) = \{\bar{b}_{2k} \cdots \bar{b}_0, \bar{b}_{2k-1} \cdots \bar{b}_{2k}, \dots, \bar{b}_1 \cdots \bar{b}_0\} = (\bar{b}_{2k} \cdots \bar{b}_0), \\ \aleph^{-1}((B'_A)) &= \aleph^{-1}((\bar{b}'_{2k} \cdots \bar{b}'_0)) = \aleph^{-1}(\{\bar{b}'_{2k} \cdots \bar{b}'_0, \bar{b}'_{2k-1} \cdots \bar{b}'_{2k}, \dots, \bar{b}'_1 \cdots \bar{b}'_0\}) = \{b'_0 \cdots b'_{2k}, b'_{2k} \cdots b'_{2k-1}, \dots, b'_1 \cdots b'_0\} = (b'_0 \cdots b'_{2k}), \end{aligned}$$

where  $(b_0 \cdots b_{2k}) \in L_k/\pi$  and  $(b'_0 \cdots b'_{2k}) \in L_{k+1}/\pi$ . This establishes (i).

Every horizontal edge  $v\aleph_\pi(v)$  of  $M_k/\pi$  has  $v \in L_k/\pi$  represented by  $\bar{b}_k \cdots \bar{b}_1 0 b_1 \cdots b_k$  in  $L_k$ , (so  $v = (\bar{b}_k \cdots \bar{b}_1 0 b_1 \cdots b_k)$ ). There are  $2^k$  such vertices in  $L_k$  and at most  $2^k$  corresponding vertices in  $L_k/\pi$ . For example,  $(0^{k+1}1^k)$  and  $(0(01)^k)$  are endpoints in  $L_k/\pi$  of two horizontal edges of  $M_k/\pi$ , each. To prove that this implies (ii), we have to see that there cannot be more than two representatives  $\bar{b}_k \cdots \bar{b}_1 b_0 b_1 \cdots b_k$  and  $\bar{c}_k \cdots \bar{c}_1 c_0 c_1 \cdots c_k$  of a vertex  $v \in L_k/\pi$ , with  $b_0 = 0 = c_0$ . Such a  $v$  is expressible as  $v = (d_0 \cdots b_0 d_{i+1} \cdots d_{j-1} c_0 \cdots d_{2k})$ , with  $b_0 = d_i$ ,  $c_0 = d_j$  and  $0 < j - i \leq k$ . Let the substring  $\sigma = d_{i+1} \cdots d_{j-1}$  be said  $(j - i)$ -feasible. Let us see that every  $(j - i)$ -feasible substring  $\sigma$  forces in  $L_k/\pi$  only vertices  $\omega$  leading to two different (parallel) horizontal edges in  $M_k/\pi$  incident to  $v$ . In fact, periodic continuation mod  $n$  of  $d_0 \cdots d_{2k}$  both to the right of  $d_j = c_0$  with minimal cyclic substring  $\bar{d}_{j-1} \cdots \bar{d}_{i+1} d_{i+1} \cdots d_{j-1} 0 = P_r$  and to the left of  $d_i = b_0$  with minimal cyclic substring  $0 d_{i+1} \cdots d_{j-1} 1 \bar{d}_{j-1} \cdots \bar{d}_{i+1} = P_\phi$  yields a 2-way infinite string that winds up onto a class  $(d_0 \cdots d_{2k})$  containing such an  $\omega$ . For example, some pairs of feasible substrings  $\sigma$  and resulting vertices  $\omega$  are:

$$(\sigma, \omega) = (\emptyset, (001)), (0, (00011)), (1, (010)), (0^2, (0000111)), (01, (0010011)), (1^2, (01100)), \\ (0^3, (000001111)), (010, (00100101101)), (01^2, (00110)), (101, (01010)), (1^3, (0111000)),$$

with ‘o’ replacing  $b_0 = 0$  and  $c_0 = 0$ , and where  $k = \lfloor \frac{n}{2} \rfloor$  has successive values  $k = 1, 2, 1, 3, 3, 2, 4, 5, 2, 2, 3$ . If  $\sigma$  is a feasible substring and  $\bar{\sigma} = \aleph(\sigma)$ , then the possible symmetric substrings  $P_\phi \sigma P_r$  about  $\sigma = 0\sigma0$  in a vertex  $v$  of  $L_k/\pi$  are in order of ascending length:

$$\begin{array}{c} 0\sigma0, \\ \bar{\sigma}0\sigma\bar{\sigma}, \\ 1\bar{\sigma}0\sigma\bar{\sigma}1, \\ \sigma1\bar{\sigma}0\sigma\bar{\sigma}1\sigma, \\ 0\sigma1\bar{\sigma}0\sigma\bar{\sigma}1\sigma0, \\ \bar{\sigma}0\sigma1\bar{\sigma}0\sigma\bar{\sigma}1\sigma0\bar{\sigma}, \\ 1\bar{\sigma}0\sigma1\bar{\sigma}0\sigma\bar{\sigma}1\sigma0\bar{\sigma}1, \\ \dots, \end{array}$$

where we use again ‘0’ instead of ‘o’ for the entries immediately preceding and following the shown central copy of  $\sigma$ . The lateral periods of  $P_r$  and  $P_\phi$  determine each one horizontal edge at  $v$  in  $M_k/\pi$  up to returning to  $b_0$  or  $c_0$ , so no entry  $e_0 = 0$  of  $(d_0 \cdots d_{2k})$  other than  $b_0$  or  $c_0$  happens such that  $(d_0 \cdots d_{2k})$  has a third representative  $\bar{e}_k \cdots \bar{e}_1 0 e_1 \cdots e_k$  (besides  $\bar{b}_k \cdots \bar{b}_1 0 b_1 \cdots b_k$  and  $\bar{c}_k \cdots \bar{c}_1 0 c_1 \cdots c_k$ ). Thus, those two horizontal edges are produced solely from the feasible substrings  $d_{i+1} \cdots d_{j-1}$  characterized above.  $\square$

To illustrate Theorem 4, let  $1 < h < n$  in  $\mathbb{Z}$  be such that  $\gcd(h, n) = 1$  and let  $\lambda_h : L_k/\pi \rightarrow L_k/\pi$  be given by  $\lambda_h((a_0 a_1 \cdots a_n)) \rightarrow (a_0 a_h a_{2h} \cdots a_{n-2h} a_{n-h})$ . For each such  $h \leq k$ , there is at least one  $h$ -feasible substring  $\sigma$  and a resulting associated vertex  $v \in L_k/\pi$  as in the proof of Theorem 4. For example, starting at  $v = (0^{k+1}1^k) \in L_k/\pi$  and applying  $\lambda_h$  repeatedly produces a number of such vertices  $v \in L_k/\pi$ . If we assume  $h = 2h'$  with  $h' \in \mathbb{Z}$ , then an  $h$ -feasible substring  $\sigma$  has the form  $\sigma = \bar{a}_1 \cdots \bar{a}_{h'} a_{h'} \cdots a_1$ , so there are at least  $2^{h'} = 2^{\frac{h}{2}}$  such  $h$ -feasible substrings.

## 6 Dihedral Quotient Pseudograph $R_k$ of $M_k$

An *involution* of a graph  $G$  is a graph map  $\mathbb{N} : G \rightarrow G$  such that  $\mathbb{N}^2$  is the identity. If  $G$  has an involution, an  $\mathbb{N}$ -*folding* of  $G$  is a graph  $H$ , possibly with loops, whose vertices  $v'$  and edges or loops  $e'$  are respectively of the form  $v' = \{v, \mathbb{N}(v)\}$  and  $e' = \{e, \mathbb{N}(e)\}$ , where  $v \in V(G)$  and  $e \in E(G)$ ;  $e$  has endvertices  $v$  and  $\mathbb{N}(v)$  if and only if  $\{e, \mathbb{N}(e)\}$  is a loop of  $G$ .

Note that both maps  $\mathbb{N} : M_k \rightarrow M_k$  and  $\mathbb{N}_\pi : M_k/\pi \rightarrow M_k/\pi$  in Section 5 are involutions. Let  $\langle B_A \rangle$  denote each horizontal pair  $\{(B_A), \mathbb{N}_\pi((B_A))\}$  (as in Theorem 4) of  $M_k/\pi$ , where  $|A| = k$ . An  $\mathbb{N}$ -folding  $R_k$  of  $M_k/\pi$  is obtained whose vertices are the pairs  $\langle B_A \rangle$  and having:

- (1) an edge  $\langle B_A \rangle \langle B_{A'} \rangle$  per skew-edge pair  $\{(B_A)\mathbb{N}_\pi((B_{A'})), (B_{A'})\mathbb{N}_\pi((B_A))\}$ ;
- (2) a loop at  $\langle B_A \rangle$  per horizontal edge  $(B_A)\mathbb{N}_\pi((B_A))$ ; because of Theorem 4, there may be up to two loops at each vertex of  $R_k$ .

**Theorem 5.**  $R_k$  is a quotient pseudograph of  $M_k$  under an action  $\Upsilon : D_{2n} \times M_k \rightarrow M_k$ .

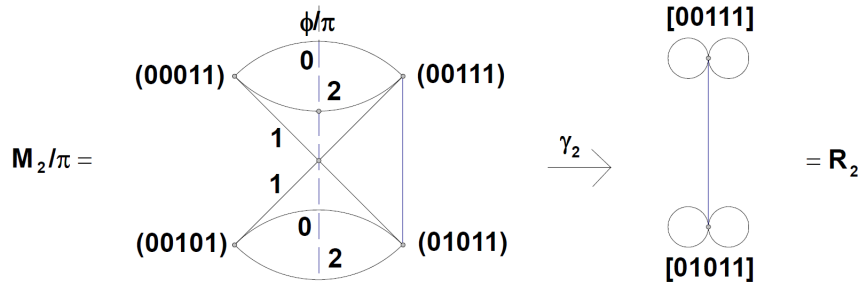


Figure 1: Reflection symmetry of  $M_2/\pi$  about a line  $\phi/\pi$  and resulting graph map  $\gamma_2$

*Proof.*  $D_{2n}$  is the semidirect product  $\mathbb{Z}_n \rtimes_\varrho \mathbb{Z}_2$  via the group homomorphism  $\varrho : \mathbb{Z}_2 \rightarrow \text{Aut}(\mathbb{Z}_n)$ , where  $\varrho(0)$  is the identity and  $\varrho(1)$  is the automorphism  $i \rightarrow (n-i)$ ,  $\forall i \in \mathbb{Z}_n$ . If  $* : D_{2n} \times D_{2n} \rightarrow D_{2n}$  indicates group multiplication and  $i_1, i_2 \in \mathbb{Z}_n$ , then  $(i_1, 0)*(i_2, j) = (i_1 + i_2, j)$  and  $(i_1, 1)*(i_2, j) = (i_1 - i_2, j)$ , for  $j \in \mathbb{Z}_2$ . Set  $\Upsilon((i, j), v) = \Upsilon'(i, \mathbb{N}^j(v))$ ,  $\forall i \in \mathbb{Z}_n, \forall j \in \mathbb{Z}_2$ , where  $\Upsilon'$  is as in display (3). Then,  $\Upsilon$  is a well-defined  $D_{2n}$ -action on  $M_k$ . By writing  $(i, j) \cdot v = \Upsilon((i, j), v)$  and  $v = a_0 \cdots a_{2k}$ , we have  $(i, 0) \cdot v = a_{n-i+1} \cdots a_{2k} a_0 \cdots a_{n-i} = v'$  and  $(0, 1) \cdot v' = \bar{a}_{i-1} \cdots \bar{a}_0 \bar{a}_{2k} \cdots \bar{a}_i = (n-i, 1) \cdot v = ((0, 1)*(i, 0)) \cdot v$ , leading to the compatibility condition  $((i, j) * (i', j')) \cdot v = (i, j) \cdot ((i', j') \cdot v)$ .  $\square$

Theorem 5 yields a graph projection  $\gamma_k : M_k/\pi \rightarrow R_k$  for the action  $\Upsilon$ , given for  $k = 2$  in Figure 1. In fact,  $\gamma_2$  is associated with reflection of  $M_2/\pi$  about the dashed vertical symmetry axis  $\phi/\pi$  so that  $R_2$  (containing two vertices and one edge between them, with each vertex incident to two loops) is given as its image. Both the representations of  $M_2/\pi$  and  $R_2$  in the figure have their edges indicated with colors 0,1,2, as arising in Section 7.

## 7 Lexical Procedure

Let  $P_{k+1}$  be the subgraph of the unit-distance graph of  $\mathbb{R}$  (the real line) induced by the set  $[k+1] = \{0, \dots, k\}$ . We draw the grid  $\Gamma = P_{k+1} \square P_{k+1}$  in the plane  $\mathbb{R}^2$  with a diagonal  $\partial$

traced from the lower-left vertex  $(0, 0)$  to the upper-right vertex  $(k, k)$ . For each  $v \in L_k/\pi$ , there are  $k + 1$   $n$ -tuples of the form  $b_0 b_1 \cdots b_{n-1} = 0 b_1 \cdots b_{n-1}$  that represent  $v$  with  $b_0 = 0$ . For each such  $n$ -tuple, we construct a  $2k$ -path  $D$  in  $\Gamma$  from  $(0, 0)$  to  $(k, k)$  in  $2k$  steps indexed from  $i = 0$  to  $i = 2k - 1$ . This leads to a lexical edge-coloring implicit in [3]; see the following statement and Figure 2 (Section 8), containing examples of such a  $2k$ -path  $D$  in thick trace.

**Theorem 6.** [3] *Each  $v \in L_k/\pi$  has its  $k + 1$  incident edges assigned colors  $0, 1, \dots, k$  by means of the following Lexical Procedure', where  $0 \leq i \in \mathbb{Z}$ ,  $w \in V(\Gamma)$  and  $D$  is a path in  $\Gamma$ . Initially, let  $i = 0$ ,  $w = (0, 0)$  and  $D$  contain solely the vertex  $w$ . Repeat  $2k$  times the following sequence of steps (1)-(3), and then perform once the final steps (4)-(5):*

- (1) *If  $b_i = 0$ , then set  $w' := w + (1, 0)$ ; otherwise, set  $w' := w + (0, 1)$ .*
- (2) *Reset  $V(D) := v(D) \cup \{w'\}$ ,  $E(D) := E(D) \cup \{ww'\}$ ,  $i := i + 1$  and  $w := w'$ .*
- (3) *If  $w \neq (k, k)$ , or equivalently, if  $i < 2k$ , then go back to step (1).*
- (4) *Set  $\check{v} \in L_{k+1}/\pi$  to be the vertex of  $M_k/\pi$  adjacent to  $v$  and obtained from its representative  $n$ -tuple  $b_0 b_1 \cdots b_{n-1} = 0 b_1 \cdots b_{n-1}$  by replacing the entry  $b_0$  by  $\bar{b}_0 = 1$  in  $\check{v}$ , keeping the entries  $b_i$  of  $v$  unchanged in  $\check{v}$  for  $i > 0$ .*
- (5) *Set the color of the edge  $v\check{v}$  to be the number  $c$  of horizontal (alternatively, vertical) arcs of  $D$  above  $\partial$ .*

*Proof.* If addition and subtraction in  $[n]$  are taken modulo  $n$  and we write  $[y, x] = \{y, y + 1, y + 2, \dots, x - 1\}$ , for  $x, y \in [n]$ , and  $S^c = [n] \setminus S$ , for  $S = \{i \in [n] : b_i = 1\} \subseteq [n]$ , then the cardinalities of the sets  $\{y \in S^c \setminus x : |[y, x] \cap S| < |[y, x] \cap S^c|\}$  yield all the edge colors, where  $x \in S^c$  varies.  $\square$

The Lexical Procedure of Theorem 6 yields a 1-factorization not only for  $M_k/\pi$  but also for  $R_k$  and  $M_k$ . This is clarified by the end of Section 8.

## 8 Lexical 1-Factorization

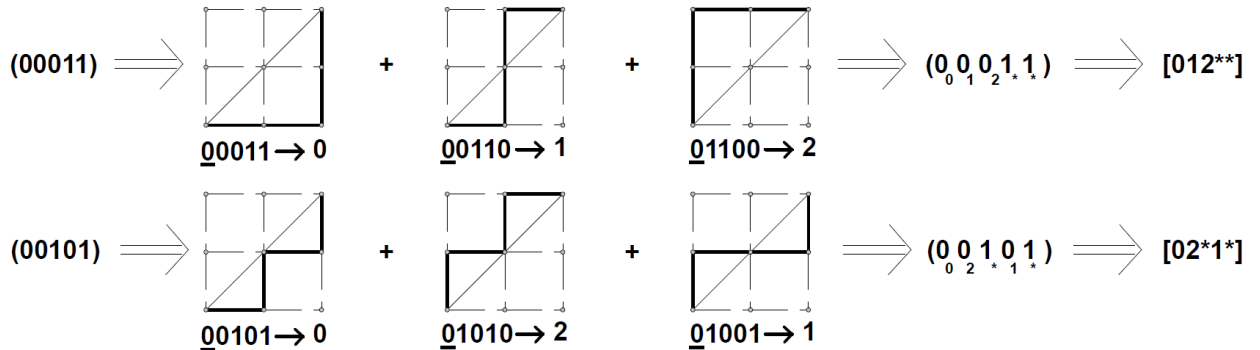


Figure 2: Representing lexical-color assignment for  $k = 2$

A notation  $\delta(v)$  is assigned to each pair  $\{v, \aleph_\pi(v)\} \in R_k$ , where  $v \in L_k/\pi$ , so that there is a unique  $k$ -germ  $\alpha = \alpha(v)$  with  $\langle F(\alpha) \rangle = \delta(v)$ , where the notation  $\langle \cdot \rangle$  appeared for example as in  $\langle B_A \rangle$  in Section 6. We exemplify  $\delta(v)$  for  $k = 2$  in Figure 2, with the Lexical Procedure

(indicated by arrows “ $\Rightarrow$ ”) departing from  $v = (00011)$  (top) and  $v = (00101)$  (bottom), passing to sketches of  $\Gamma$  (separated by symbols “+”), one sketch (in which to trace the edges of  $D \subset \Gamma$  as in Theorem 6) per representative  $b_0 b_1 \cdots b_{n-1} = 0 b_1 \cdots b_{n-1}$  of  $v$  shown under the sketch (where  $b_0 = 0$  is underscored) and pointing via an arrow “ $\rightarrow$ ” to the corresponding color  $c \in [k+1]$ . Recall this  $c$  is the number of horizontal arcs of  $D$  below  $\partial$ .

In each of the two cases in Figure 2 (top, bottom), an arrow “ $\Rightarrow$ ” to the right of the sketches points to a modification  $\hat{v}$  of  $b_0 b_1 \cdots b_{n-1} = 0 b_1 \cdots b_{n-1}$  obtained by setting as a subindex of each 0 (resp. 1) its associated color  $c$  (resp. an asterisk “\*”). Further to the right, a third arrow “ $\Rightarrow$ ” points to the  $n$ -tuple  $\delta(v)$  formed by the string of subindexes of entries of  $\hat{v}$  in the order they appear from left to right.

**Theorem 7.** *Let  $\alpha(v^0) = a_{k-1} \cdots a_1 = 00 \cdots 0$ . Each  $\delta(v)$  corresponds to a sole  $k$ -germ  $\alpha = \alpha(v)$  with  $\langle F(\alpha) \rangle = \delta(v)$  by means of the following Uncastling Procedure: Given  $v \in L_k/\pi$ , let  $W^i = 01 \cdots i$  be the maximal initial numeric (i.e., colored) substring of  $\delta(v)$ , so that the length of  $W^i$  is  $i+1$  ( $0 \leq i \leq k$ ). If  $i = k$ , let  $\alpha(v) = \alpha(v^0)$ ; else, set  $m = 0$  and:*

1. set  $\delta(v^m) = \langle W^i | X | Y | Z^i \rangle$ , where  $Z^i$  is the terminal  $j_m$ -substring of  $\delta(v^m)$ , with  $j_m = i+1$ , and let  $X, Y$  (in that order) start at contiguous numbers  $\Omega$  and  $\Omega-1 \geq i$ ;
2. set  $\delta(v^{m+1}) = \langle W^i | Y | X | Z^i \rangle$ ;
3. obtain  $\alpha(v^{m+1})$  from  $\alpha(v^m)$  by increasing its entry  $a_{j_m}$  by 1;
4. if  $\delta(v^{m+1}) = [01 \cdots k * \cdots *]$ , then stop; else, increase  $m$  by 1 and go to step 1.

*Proof.* This is a procedure inverse to that of castling (Section 3), so 1-4 follow.  $\square$

Theorem 7 allows to produce a finite sequence  $\delta(v^0), \delta(v^1), \dots, \delta(v^m), \dots, \delta(v^s)$  of  $n$ -strings with  $j_0 \geq j_1 \geq \cdots \geq j_m \cdots \geq j_{s-1}$  as in steps 1-4, and  $k$ -germs  $\alpha(v^0), \alpha(v^1), \dots, \alpha(v^m), \dots, \alpha(v^s)$ , taking from  $\alpha(v^0)$  through the  $k$ -germs  $\alpha(v^m)$ , ( $m = 1, \dots, s-1$ ), up to  $\alpha(v) = \alpha(v^s)$  via unit incrementation of  $a_{j_m}$ , for  $0 \leq m < s$ , where each incrementation yields the corresponding  $\alpha(v^{m+1})$ . Recall  $F$  is a bijection from the set  $V(\mathcal{T}_k)$  of  $k$ -germs onto  $V(R_k)$ , both sets being of cardinality  $C_k$ . Thus, to deal with  $V(R_k)$  it is enough to deal with  $V(\mathcal{T}_k)$ , a fact useful in interpreting Theorem 8 below. For example  $\delta(v^0) = \langle 04 * 3 * 2 * 1 * \rangle = \langle 0 | 4 * | 3 * 2 * 1 | * \rangle = \langle W^0 | X | Y | Z^0 \rangle$  with  $m = 0$  and  $\alpha(v^0) = 123$ , continued in Table III with  $\delta(v^1) = \langle W^0 | Y | X | Z^0 \rangle$ , finally arriving to  $\alpha(v^s) = \alpha(v^6) = 000$ .

**Table III.** Continuation of the Uncastling Procedure started at  $\alpha(v^0) = 123$ .

$j_0=0$	$\delta(v^1)$	$=$	$\langle 0   3 * 2 * 1   4 *   * \rangle$	$=$	$\langle 03 * 2 * 14 * * \rangle$	$=$	$\langle 0   3 *   2 * 14 *   * \rangle$	$\alpha(v^1)=122$	$\langle F(122) \rangle = \delta(v^1)$
$j_1=0$	$\delta(v^2)$	$=$	$\langle 0   2 * 14 *   3 *   * \rangle$	$=$	$\langle 02 * 14 * 3 * * \rangle$	$=$	$\langle 0   2 *   14 * 3 *   * \rangle$	$\alpha(v^2)=121$	$\langle F(121) \rangle = \delta(v^2)$
$j_2=0$	$\delta(v^3)$	$=$	$\langle 0   14 * 3 *   2 *   * \rangle$	$=$	$\langle 014 * 3 * 2 * * \rangle$	$=$	$\langle 01   4 *   3 * 2   * * \rangle$	$\alpha(v^3)=120$	$\langle F(120) \rangle = \delta(v^3)$
$j_3=1$	$\delta(v^4)$	$=$	$\langle 01   3 * 2   4 *   * * \rangle$	$=$	$\langle 013 * 24 * * * \rangle$	$=$	$\langle 01   3 *   24 *   * * \rangle$	$\alpha(v^4)=110$	$\langle F(110) \rangle = \delta(v^4)$
$j_4=1$	$\delta(v^5)$	$=$	$\langle 01   24 *   3 *   * * \rangle$	$=$	$\langle 0124 * 3 * * * \rangle$	$=$	$\langle 012   4 *   3   * * \rangle$	$\alpha(v^5)=100$	$\langle F(100) \rangle = \delta(v^5)$
$j_5=2$	$\delta(v^6)$	$=$	$\langle 012   3   4 *   * * * \rangle$	$=$	$\langle 01234 * * * \rangle$			$\alpha(v^6)=000$	$\langle F(000) \rangle = \delta(v^6)$

A pair of skew edges  $(B_A) \aleph_\pi((B_{A'}))$  and  $(B_{A'}) \aleph((B_A))$  in  $M_k/\pi$ , to be called a *skew reflection edge pair (SREP)*, provides a color notation for any  $v \in L_{k+1}/\pi$  such that in each particular edge class mod  $\pi$ :

- (I) all edges receive a common color in  $[k+1]$  regardless of the endpoint on which the Lexical Procedure (or its modification immediately below) for  $v \in L_{k+1}/\pi$  is applied;
- (II) the two edges in each SREP in  $M_k/\pi$  are assigned a common color in  $[k+1]$ .

The modification in step (I) consists in replacing in Figure 2 each  $v$  by  $\aleph_\pi(v)$  so that on the left we have instead now (00111) (top) and (01011) (bottom) with respective sketch subtitles

$$\begin{array}{lll} 00111 \rightarrow 0, & 10011 \rightarrow 1, & 11001 \rightarrow 2, \\ 01011 \rightarrow 0, & 10101 \rightarrow 2, & 01101 \rightarrow 1, \end{array}$$

resulting in similar sketches when the steps (1)-(5) of the Lexical Procedure are taken with right-to-left reading and processing of the entries on the left side of the subtitles (before the arrows “ $\rightarrow$ ”), where the values of each  $b_i$  must be taken complemented, (i.e., as  $\bar{b}_i$ ).

Since an SREP in  $M_k$  determines a unique edge  $\epsilon$  of  $R_k$  (and vice versa), the color received by the SREP can be attributed to  $\epsilon$ , too. Clearly, each vertex of either  $M_k$  or  $M_k/\pi$  or  $R_k$  defines a bijection from its incident edges onto the color set  $[k+1]$ . The edges obtained via  $\aleph$  or  $\aleph_\pi$  from these edges have the same corresponding colors.

**Theorem 8.** *A 1-factorization of  $M_k/\pi$  by the colors  $0, 1, \dots, k$  is obtained via the Lexical Procedure and can be lifted to a covering 1-factorization of  $M_k$  and subsequently collapsed onto a folding 1-factorization of  $R_k$ . This validates the notation  $\delta(v)$ , for each  $v \in V(R_k)$ , so that there is a unique  $k$ -germ  $\alpha = \alpha(v)$  with  $\langle F(\alpha) \rangle = \delta(v)$ .*

*Proof.* As pointed out in (II) above, each SREP in  $M_k/\pi$  has its edges with a common color in  $[k+1]$ . Thus, the  $[k+1]$ -coloring of  $M_k/\pi$  induces a well-defined  $[k+1]$ -coloring of  $R_k$ . This yields the claimed collapsing to a folding 1-factorization of  $R_k$ . The lifting to a covering 1-factorization in  $M_k$  is immediate. The arguments above determine that the collapsing 1-factorization in  $R_k$  induces the claimed  $k$ -germs  $\alpha(v)$ .  $\square$

## 9 Binary Tree for the $k$ -germs $\alpha$ and their $F(\alpha)$ 's, $\forall 0 < k$

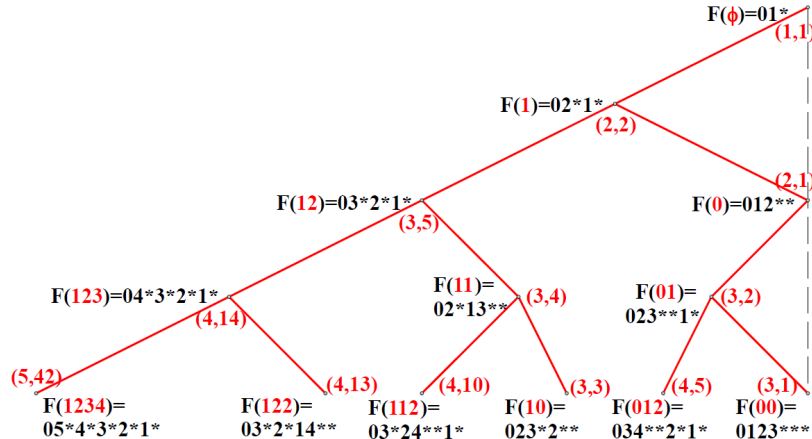


Figure 3: Restriction of  $T$  to its first five levels

The graph  $R_1$  has just one vertex 001 with  $\delta(001) = 01*$  ( $\delta$  as in Section 8) and two loops. Note that the correspondence  $F$  in Section 3 has  $01*$  as the image of the empty set:  $F(\emptyset) = 01*$ . While Theorem 3 allows to sort all  $k$ -germs for a fixed  $k$ , the following theorem allows to sort all  $k$ -germs.

**Theorem 9.** A binary tree  $T$  exists with node set  $\cup_{k=1}^{\infty} V(R_k)$  and such that: **(A)** its root is  $01*$ ; **(B)** the left child of a node  $\delta(v) = 0|X$  in  $T$  with  $||X|| = 2k$  ( $||X|| = \text{length of } X$ ) exists and is  $0|X + 1|1*$ , where  $X + 1 = (x_1 + 1) \cdots (x_{2k} + 1)$  if  $X = x_1 \cdots x_{2k}$  with color number addition and  $* + 1 = *$ ; **(C)** unless  $\delta(v) = 01 \cdots (k-1)k * \cdots *$ , it is  $\delta(v) = 0|X|Y*$ , where  $X$  and  $Y$  are strings starting at some  $j > 1$  and  $j-1$ , respectively, in which case there is a right child of  $\delta(v)$ , namely  $0|Y|X|*$ , via uncastling. In terms of  $k$ -germs,  $T$  has each node  $a_{k-1}a_{k-2} \cdots a_2a_1$  as a parent of a left child  $b_kb_{k-1} \cdots b_1 = a_{k-1}a_{k-2} \cdots a_2a_1(a_1 + 1)$ , and as a parent of a right child  $\rho$  only if  $a_1 > 0$ , in which case  $\rho = c_{k-1} \cdots c_2c_1 = a_{k-1} \cdots a_2(a_1 - 1)$ .

*Proof.* Figure 3 shows the first five levels of  $T$  with edges in red and nodes, expressed in terms of red  $k$ -germs via  $F$ , in otherwise black equalities. To stress the claimed unifying pattern mentioned in Section 1, the figure also assigns to each node a red-colored ordered pair of positive integers  $(i, j)$ , where  $j \leq C_i$ . The root, given by  $F(\emptyset) = 01*$ , is assigned red  $(i, j) = (1, 1)$ . The left child of a node assigned red  $(i, j)$  is assigned red  $(k, j') = (i + 1, j')$ , where  $j'$  is the order of appearance of the  $k$ -germ  $\alpha$  corresponding to  $(k, j')$  in its presentation via castling as in Table I;  $\alpha$  becomes the  $k$ -germ corresponding to  $j'$  in the sequence  $\mathcal{S}$  ([A239903](#)), once the extra zeros to the left of its leftmost nonzero entry are removed. Note  $j' = j'(j)$  arises from the series associated to [A076050](#), deducible from items 1-4 in Section 16. The right child of a red  $(i, j)$  is defined only if  $j > 1$  (strictly to the left of the vertical dotted line); in that case, it is assigned red  $(i, j - 1)$ .  $\square$

## 10 Comparing $k$ -Germs and $k$ -RGS's

We show now that the  $k$ -germs of Section 2, that were used in all of the above, are equivalent to the sequences of item (u) page 224 [[10](#)]. These sequences, that we call  $k$ -RGS's in the present context to distinguish them from our  $k$ -germs, are indicated in the form  $a_0a_1 \cdots a_{k-1}$  satisfying  $a_0 = 0$  and  $0 \leq a_{i+1} \leq a_i + 1$ . Item (r) page 224 [[10](#)] can be used to show that these  $k$ -RGS's represent bijectively the  $k$ -edge ordered trees, also presented in item (e) page 221 [[10](#)]. In fact, let  $b_i = a_i - a_{i+1} + 1$  and replace  $a_i$  with one “1” followed by  $b_i$  “-1”s, for  $1 \leq i \leq k-1$ , where we assume  $a_k = 0$ , to get a sequence as in item (r), i.e. sequences of  $k-1$  “1”s and  $k-1$  “-1”s such that every partial sum is nonnegative, with “-1” denoted simply as “-”.

TABLE III

<u>01</u> <sup>1</sup> <u>00</u> <sup>2</sup> 10 <sup>1</sup> 11 <sup>1</sup> <u>12</u>	<u>012</u> <sup>1</sup> 011 <sup>1</sup> 010 <sup>2</sup> <u>000</u> <sup>3</sup> 100 <sup>2</sup> 110 <sup>2</sup> 120 <sup>1</sup> 121 <sup>1</sup> 122 <sup>1</sup> <u>123</u>
<u>10</u> <sup>1</sup> <u>12</u> <sup>2</sup> 11 <sup>1</sup> 01 <sup>1</sup> <u>00</u>	<u>100</u> <sup>1</sup> 012 <sup>1</sup> 121 <sup>2</sup> <u>123</u> <sup>3</sup> 122 <sup>2</sup> 112 <sup>2</sup> 111 <sup>1</sup> 011 <sup>1</sup> 001 <sup>1</sup> <u>000</u>

For a bijection of the  $k$ -edge ordered trees with the sequence in item (r), a depth-first (preorder) search through each  $k$ -edge ordered tree is performed: When going “down” an edge (away from the root) records a “1”, and when going “up” an edge records a “-1”. Thus,

the  $k$ -germs are in 1-1 correspondence with the RGS's, as claimed. However, each  $k$ -germ and its correspondent  $k$ -RGS have different expressions, as can be seen by comparing, in the pair of graph subtables in TABLE III, the tree  $\mathcal{T}_k$  presented with its nodes expressed first as  $k$ -germs (top table) and then as  $k$ -RGS's (bottom table), for  $k = 3, 4$ , where the root is doubly underlined and the leaves are simply underlined, and where  $k$ -RGS's are written  $a_1 \cdots a_{k-1}$  instead of  $a_0 a_1 \cdots a_{k-1} = 0 a_1 \cdots a_{k-1}$ :

TABLE IV

$i$	$edge\ label$ $subseq\ of\ \ell_i$	$first$ $node\ in\ \ell_i$	$2nd$ $node\ in\ \ell_i$	$etc.$	$etc.$	$etc.$	$etc.$	$etc.$
1	$k_1$	$01 \dots k_3 k_2 k_1$	$01 \dots k_3 k_2^2$	—	—	—	—	—
2	$k_2^2$	$01 \dots k_3 k_2^2$	$01 \dots k_3^2 k_2$	$01 \dots k_4 k_3^3$	—	—	—	—
3	$k_3^3$	$01 \dots k_4 k_3^3$	$01 \dots k_4^2 k_3^2$	$01 \dots k_4^3 k_3$	$01 \dots k_4^4$	—	—	—
...	...	...	...	...	...	—	—	—
$j$	$k_j^j$	$01 \dots k_{j+1} k_j^j$	$01 \dots k_{j+1}^2 k^{j_1}$	$01 \dots k_{j+1}^3 k_j^{j_2}$	...	$01 \dots k_j^j$	—	—
...	...	...	...	...	...	...	—	—
$k_3$	3	$0123^{k_3}$	$012^2 3^{k_4}$	$012^3 3^{k_5}$	...	$012^{k_2}$	—	—
$k_2$	2	$012^{k_2}$	$01^2 2^{k_3}$	$01^3 2^{k_4}$	...	$01^{k_2} 2$	$01^{k_1}$	—
$k_1$	1	$01^{k_1}$	$0^2 1^{k-2}$	$0^3 1^{k_3}$	...	$0^{k_2} 1^2$	$0^{k_1} 1$	$0^k$

In these representations of  $\mathcal{T}_k$  each edge is given as a short segment with a label  $i = i(\alpha)$  as in Theorem 2. Thus, each path from the root to a leaf in  $\mathcal{T}_k$  can be presented by the associated subsequence of edge labels. From the tables above, we see that the collection of such subsequences for  $k = 3$  is  $\{211, 1\}$ , and for  $k = 4$  is  $\{322111, 3211, 31, 211\}$ .

Let  $\chi$  be the assignment that to each  $k$ -germ  $\alpha$  assigns its associated  $k$ -RGS. Expressing  $k$ -RGS's as  $a_0 a_1 \cdots a_{k-1} = 0 a_1 \cdots a_{k-1}$ , for example  $k = 3$  yields

$$\chi(\underline{00}) = \underline{012}, \quad \chi(\underline{01}) = \underline{010}, \quad \chi(10) = 011, \quad \chi(11) = 001, \quad \chi(\underline{12}) = \underline{000}.$$

The lower table above can be taken to represent the trees  $\chi(\mathcal{T}_3)$  and  $\chi(\mathcal{T}_4)$ .

TABLE V

							<u>0000</u>
							<u>0010</u> <u>0001</u>
							<u>0110</u> <u>0101</u> <u>0011</u>
							<u>1230</u> <u>1220</u> <u>1120</u> <u>1110</u> <u>1101</u> <u>1011</u> <u>0111</u>
							<u>1211</u> <u>1123</u> <u>1232</u> <u>1234</u> <u>1233</u> <u>1223</u> <u>1222</u> <u>1122</u> <u>1112</u> <u>1111</u>
							<u>0121</u> <u>1201</u> <u>1210</u> <u>1231</u> <u>1221</u> <u>1212</u> <u>1121</u> <u>0112</u> <u>1001</u> <u>0100</u>
							<u>0012</u> <u>0120</u> <u>0123</u> <u>0122</u> <u>1012</u>
							<u>1000</u> <u>1200</u> <u>1100</u> <u>1010</u>

The following properties are seen to hold for  $1 < k \in \mathbb{Z}$ :

1. The root of  $\chi(\mathcal{T}_k)$  and its farthest leaf in  $\chi(\mathcal{T}_i)$  are  $\chi(0^{k-1}) = 012 \cdots (k-1)$  and  $\chi(12 \cdots (k-1)) = 0^k$ . Furthermore, the leaves of  $\chi(\mathcal{T}_k)$  are those RGS's  $a_0 a_1 \cdots a_{k-1}$  with  $a_{k-1} = 0$ .
2. Each maximum path  $\ell_i$  of  $\chi(\mathcal{T}_k)$  whose edges have a constant label  $i \in [1, n]$  has initial and terminal nodes of the form  $A_1 = 0a_1 a_2 \cdots a_n$  and  $A_h = 0(a_2 - 1) \cdots (a_n - 1)(i - 1)$ .
3. By writing  $k_j = k - j$ , for  $j = 1, \dots, k-1$ , the longest path  $\ell$  in  $\chi(\mathcal{T}_k)$  departing from its root has associated edge-label sequence  $k_1 k_2^2 k_3^3 \cdots k_j^j \cdots 2^{k_2} 1^{k_1}$  and is the result of concatenating successively its subpaths  $\ell_i$  as in item 2, described in Table IV.
4. Each node  $A$  of  $\chi(\mathcal{T}_{k+1})$  that is a  $(k+1)$ -RGS's having a maximal substring of the form  $012 \dots j$  of length  $j+1$ , where  $j$  is the sole maximum entry in  $A$ , yields a node of  $\chi(\mathcal{T}_k)$  by just removing  $j$  from  $A$ . All such nodes  $A$  of  $\chi(\mathcal{T}_{k+1})$  yield, by these indicated removals, all of  $\chi(\mathcal{T}_k)$ . To be used below, let  $\chi''_{k+1}$  be the set of all the nodes  $A$  above in this item and let  $\chi'_{k+1} = \chi(\mathcal{T}_{k+1}) \setminus \chi''_{k+1}$ .
5. Let  $(A_1, A_2, \dots, A_h)$  be a path as in item two in  $\chi'_{k+1} \setminus \ell$ . To obtain  $A_{i-1}$  from  $A_i = 0a_1 \cdots a_{k-1}$ , for  $i = h, h-1, \dots, 2$ , let  $A_i = A'_i | A''_i$  be obtained by the concatenation of the strings  $A'_i = a_0 a_1 \cdots a_j$  and  $A''_i = a_{j+1} \cdots a_{k-1}$ , where  $A'_i = a_0 = 0$ , if  $a_1 = 0$ , and  $A'_i$  is the maximal initial nondecreasing substring of  $A_i$ , otherwise, and where  $A''_i = A_i \setminus A'_i$ . Then  $A_{i-1} = 0 | (A''_i \setminus a_{j+1}) | (A'_i + 1) = 0a_{j+2} \cdots a_{k-1}(a_0 + 1)(a_1 + 1) \cdots (a_j + 1)$ .

Tables V and VI contain respective representations of  $\chi(\mathcal{T}_5)$  and  $\chi''_6$ , the latter one here with a bar over the maximal entry of each RGS node, as in item 4, entry whose removal yields a corresponding node of  $\chi(\mathcal{T}_4)$ .

TABLE VI

							<u>10000</u>
							<u>00120</u> <u>00012</u>
							<u>01210</u> <u>01201</u> <u>00121</u>
							<u>12340</u> <u>12320</u> <u>11230</u> <u>12110</u> <u>12101</u> <u>12011</u> <u>01211</u>
							<u>12311</u> <sup>2</sup> <u>11234</u> <sup>2</sup> <u>12342</u> <sup>3</sup> <u>12345</u> <sup>4</sup> <u>12343</u> <sup>3</sup> <u>12234</u> <sup>3</sup> <u>12322</u> <sup>2</sup> <u>11232</u> <sup>2</sup> <u>11123</u> <sup>2</sup> <u>12111</u>
							<u>01231</u> <u>12301</u> <u>12310</u> <u>12341</u> <u>12321</u> <u>12312</u> <sup>2</sup> <u>11231</u> <sup>1</sup> <u>01123</u> <sup>1</sup> <u>12001</u> <sup>1</sup> <u>01200</u>
							<u>00123</u> <u>01230</u> <u>01234</u> <u>01232</u> <u>10123</u>
							<u>12000</u> <u>12300</u> <u>12100</u> <u>12010</u>

As an additional example here, Table VII contains a representation of  $\chi'_6$ .

TABLE VII

<u>10122<sup>1</sup>11010</u>											
<u>12200 11200 11100 12212<sup>2</sup>11221<sup>1</sup>01122<sup>1</sup>11001<sup>1</sup>01100</u>										<u>00100</u>	
<u>01233 01223 01222 11012<sup>1</sup>10110</u>										<u>00100</u>	
<u>12345 12331 12231 12221 12122<sup>2</sup>11212<sup>2</sup>11121<sup>1</sup>01112<sup>1</sup>10011<sup>1</sup>01001</u>										<u>00100</u>	
<u>12211<sup>2</sup>11233<sup>2</sup>12332<sup>3</sup>12344<sup>4</sup>12334<sup>4</sup>12333<sup>3</sup>12233<sup>3</sup>12223<sup>3</sup>12222<sup>2</sup>11222<sup>2</sup>11122<sup>2</sup>11112<sup>2</sup>11111</u>										<u>00100</u>	
<u>01221 12201 12210 12330 12220 11220 11120 11110 11101 11011 10111 01111</u>										<u>00100</u>	
<u>00122 01220 12120<sup>1</sup>12323<sup>2</sup>12123<sup>2</sup>12121 01110 01101 01011 00111</u>										<u>00100</u>	
<u>11000 11210<sup>1</sup>12232 12012 01212 00110 00101 00011</u>										<u>00010 00001</u>	
<u>01120<sup>1</sup>11201<sup>1</sup>11223 10120 10012<sup>1</sup>10100 00010 00001</u>										<u>00000</u>	
<u>10010<sup>1</sup>01012<sup>1</sup>10121<sup>1</sup>12112<sup>2</sup>11211<sup>1</sup>01121<sup>1</sup>00112<sup>1</sup>10001<sup>1</sup>01000</u>										<u>00000</u>	

By considering the order-number permutations (as in the left column in Table I above) via  $\chi$  we obtain permutations as follows:

$k = 3$	$(0, 4)(1, 2, 3)$
$k = 4$	$(0, 13)(1, 8, 6, 7, 9, 2, 11, 3, 4, 5, 12)$
$k = 5$	$(0, 41)(1, 37, 22, 18, 19, 36, 2, 38, 8, 29, 21, 32, 7, 27, 5, 39, 3, 13, 14, 40)$ $(4, 28, 35, 6, 30, 26, 15, 33, 23, 16, 34, 17, 12)(9, 10, 31, 20, 24, 25)(11)$

## 11 Stepwise-Reversing View of the 2-Factor $W_{01}^k$

Given a  $k$ -germ  $\alpha$ , let  $(\alpha)$  represent the dihedral class  $\delta(v) = \langle F(\alpha) \rangle$  with  $v \in L_k/\pi$ . Recall  $W_{01}^k$  is the 2-factor given by the union of the 1-factors of colors 0, 1 in  $M_k$  (namely those formed by lifting the edges  $\alpha\alpha^0, \alpha\alpha^1$  of  $R_k$  in the notation of Section 14, instead of those of colors  $k, k-1$ , as in [2]). The cycles of  $W_{01}^k$  are grown in this section from specific paths, suggested in Figure 4 for  $k = 2, 3, 4$  (say: cycle  $C_0$  starting with vertically expressed path  $X(0)$ , for  $k = 2$ ; cycles  $C_0, C_1$  starting with vertically expressed paths  $X(0), X(1)$ , for  $k = 3$ ; and cycles  $C_0, C_1, C_2$  starting with vertically expressed paths  $X(0), X(1), X(2)$ , for  $k = 4$ ). Here, vertices  $v \in L_k$  (resp.  $v \in L_{k+1}$ ) are represented with:

- (a) 0- (resp. 1-) entries replaced by their respective colors  $0, 1, \dots, k$  (resp. asterisks);
- (b) 1- (resp. 0-) entries replaced by asterisks (resp. their respective colors  $0, 1, \dots, k$ );
- (c) delimiting chevron symbols " $>$ " or " $\rangle$ " (resp. " $<$ " or " $\langle$ "), instead of parentheses or brackets, indicating the reading direction of "*forward*" (resp. "*backward*")  $n$ -tuples, effectively showing the stepwise-reversing character of the path presentations.

Each such  $v$  belongs (via the set membership symbol expressed by " $\varepsilon$ " in Figure 4) to  $(\alpha_v)$ , where  $\alpha_v$  is the  $k$ -germ of  $v$ , also expressed as its (underlined decimal) natural order. In each case, Figure 4 shows a vertically presented path  $X(i)$  of length  $4k-1$  in the corresponding

cycle  $C_i$  starting at the vertex  $w = b_0b_1 \cdots b_{2k} = 01 \cdots *$  of smallest natural order and proceeding by traversing the edges colored 1 and 0, alternatively. The terminal vertex of such subpath is  $b_{2k}b_0b_1 \cdots b_{2k-1} = *01 \cdots b_{2k-1}$ , obtained by translation mod  $n$  from  $w$ .

**Observation 10.** *The initial entries of the vertices in each  $C_i$  are presented downward, first in the 0-column of  $X(i)$ , then in the  $(2k-j)$ -column of  $X(i)$ , ( $j \in [2k]$ , only up to  $|C_i|$ ).*

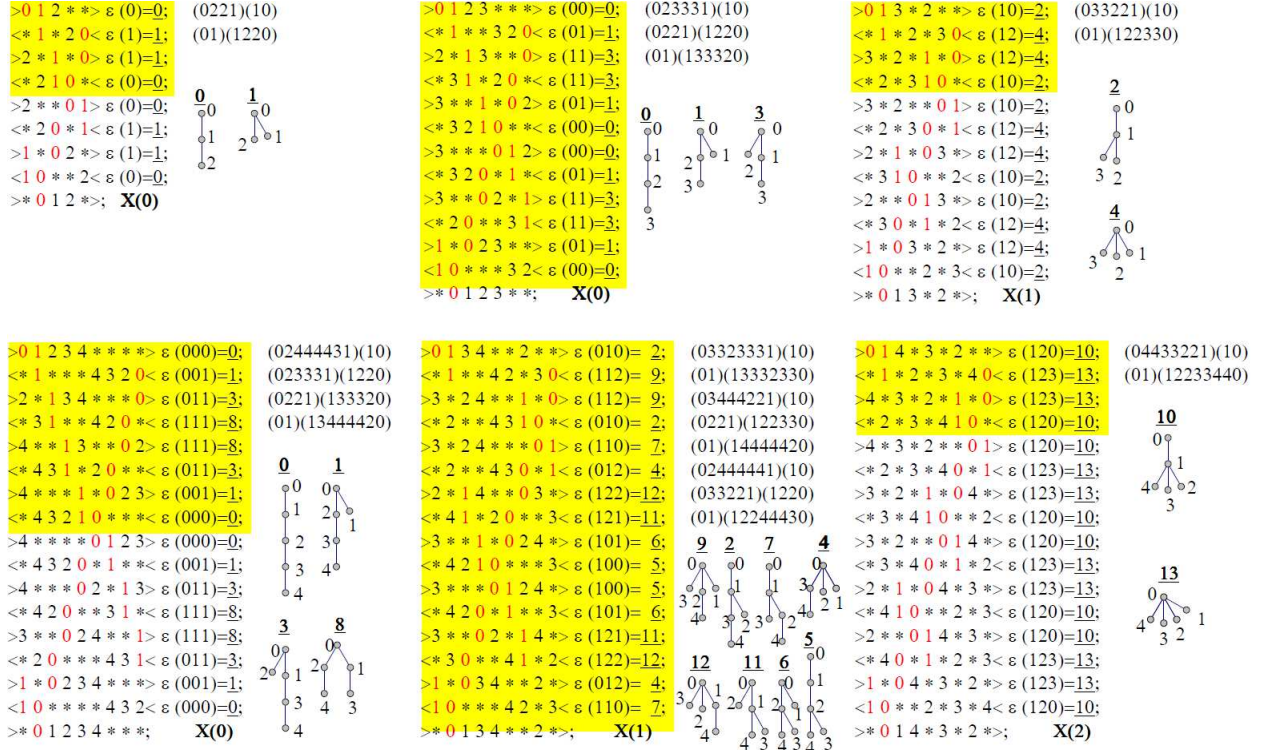


Figure 4: Cycles of  $W_{01}^k$  in  $M_k$ , ( $k = 2, 3, 4$ )

In Figure 4, initial entries are red if they are in  $\{0, 1\}$  and each cycle  $C_i$  is encoded on its top right by a vertical sequence of expressions  $(0 \cdots 1)(1 \cdots 0)$  that allows to get the sequence of initial entries of the succeeding vertices of  $C_i$  by interspersing asterisks between each two terms inside parentheses  $(\cdot)$ , then removing those  $(\cdot)$ . A  $k$ -edge ordered tree  $T = T_v$  (Proposition 1) for each  $v$  in the exemplified  $C_i$  ( $= C$  in Proposition 2(v) [2]) is shown at the lower right of its case in Figure 4. Each of these  $T_v$  for a specific  $C_i$  corresponds to the  $k$ -germ  $\alpha_v$  (so we write  $F(\alpha_v) = F(T_{\alpha_v})$ ) and is headed in the figure by its (underlined decimal) natural order. In the figure, vertices of each  $T_v$  are denoted  $i$ , instead of  $v_i$  ( $i \in [k+1]$ ). The trees corresponding to the  $k$ -germs in each case are obtained by applying *root rotation* [2], consisting in replacing the tree root by its leftmost child and redrawing the ordered tree accordingly. A *plane tree* is an equivalence relation of ordered trees under root rotations. In the notation of Section 14, applying one root rotation has the same effect as traversing first an edge  $\alpha\alpha_0$  in  $C_i$  and then edge  $\beta\beta_1$ , also in  $C_i$ , where  $\beta = \alpha_0$ . In each case, a yellow box shows a subpath of  $X(i)$  with  $\frac{1}{n}|V(C_i)|$  vertices of  $C_i$  that takes into account the rotation symmetry of the associated plane tree  $\mathcal{T}_i$ . In Figure 4 for  $k = 4$ , successive application of

root rotations on the second cycle,  $C_1$ , produces the cycle  $(\underline{9}, \underline{2}, \underline{4}, \underline{11}, \underline{5}, \underline{6}, \underline{12}, \underline{7})$ , the square graph of  $C_1$ , that starts downward from the second row or upward from the third row, thus covering respectively the vertices of  $L_4$  or  $L_5$  in the class. Let  $D_i$  ( $i \geq 0$ ) be the set of substrings of length  $2i$  in an  $F(\alpha)$  with exactly  $i$  color-entries such that in every prefix (i.e. initial substring), the number of asterisk-entries is at least as large as the number of color-entries. The elements of  $D = \bigcup_{i \geq 0} D_i$  are known as *Dyck words*. Each  $F(\alpha)$  is of the form  $0v1u*$ , where  $u$  and  $v$  are Dyck words and 0 and 1 are colors in  $[k+1]$  [2]. The “forward”  $n$ -tuple  $F(\alpha)$  in  $(\underline{9}, \underline{2}, \underline{4}, \underline{11}, \underline{5}, \underline{6}, \underline{12}, \underline{7})$  can be written with parentheses enclosing such Dyck words  $v$  and  $u$ , namely  $0()1(34 * * 2 * *)*$ , for  $\underline{2}$ ;  $0(3 * 24 * *)1()*$ , for  $\underline{9}$ ;  $0()1(3 * 24 * *)*$ , for  $\underline{7}$ ;  $0(3 * 2 * *)1(4 * *)*$ , for  $\underline{12}$ ;  $0(24 * 3 * *)1()*$ , for  $\underline{6}$ ;  $0()1(24 * 3 * *)*$ , for  $\underline{5}$ ;  $0(2 * *)1(4 * 3 * *)*$ , for  $\underline{11}$ ; and  $0(34 * * 2 * *)1()*$ , for  $\underline{4}$ . Similar treatment holds for “backward”  $n$ -tuples. As in Figure 4, each pair  $(0 \cdots 1)(1 \cdots 0)$  represents two paths in the corresponding cycle, of lengths  $2|(0 \cdots 1)| - 1$  and  $2|(1 \cdots 0)|$ , adding up to  $4k + 2$ . If these two paths are of the form  $0v1u*$  and  $0v'1u'*$  (this one read in reverse), then  $|u| + 2 = |(0 \cdots 1)|$  and  $|u'| + 2 = |(1 \cdots 0)|$ . (In the representations in Section 15, the first path here moves downward and the second path moves upward). Reading these paths starts at a 0-entry and ends at a 1-entry. In reality, the collections of paths obtained from the 1-factors here have the leftmost entry of the  $n$ -tuples representing their vertices constantly equal to  $1 \in \mathbb{Z}_2$  before taking into consideration (items (a) and (b) above, but with the reading orientations given in item (c)).

The 1-factor of color 0 makes the endvertices of each of its edges to have their representative plane trees obtained from each other by *horizontal reflection*  $\Phi = F\alpha^0F^{-1}$ . For example, Figure 4 shows that for  $k = 2$ : both  $\underline{0}, \underline{1}$  in  $X(0)$  are fixed via  $\Phi$ ; for  $k = 3$ :  $\underline{0}$  in  $X(0)$  is fixed via  $\Phi$  and  $\underline{1}, \underline{3}$  in  $X(0)$  correspond to each other via  $\Phi$ ; and  $\underline{2}, \underline{4}$  in  $X(1)$  are fixed via  $\Phi$ ; for  $k = 4$ :  $\underline{0}, \underline{8}$  in  $X(0)$  are fixed via  $\Phi$  and  $\underline{1}, \underline{3}$  in  $X(0)$  correspond to each other via  $\Phi$ ;  $\underline{5}, \underline{9}$  in  $X(1)$  are fixed via  $\Phi$  and the pairs  $(\underline{5}, \underline{9}), (\underline{2}, \underline{7}), (\underline{4}, \underline{12})$  and  $(\underline{6}, \underline{11})$  in  $X(1)$  are pairs of correspondent plane trees via  $\Phi$ ; and  $\underline{10}, \underline{13}$  in  $X(2)$  are fixed via  $\Phi$ . This horizontal reflection symmetry arises from Theorem 4. It accounts for each pair of contiguous rows in any  $X(i)$  corresponding to a 0-colored edge. For  $k = 5$ , this symmetry via  $\Phi$  occurs in all cycles  $C_i$  ( $i \in [6]$ ). But we also have  $F(\underline{22}) \Rightarrow 024 * * 135 * **$ , where  $\underline{22} = (1111)$  in  $C_0$  and  $F(\underline{39}) \Rightarrow 03 * 2 * 15 * 4 * **$ , where  $\underline{39} = (1232)$  in  $C_3$ , both having their 1-colored edges leading to reversed reading between  $L_5$  and  $L_6$ , again by Theorem 4. Moreover,  $F((11 \cdots 1))$  has a similar property only if  $k$  is odd; but if  $k$  is even, a 0-colored edge takes place, instead of the 1-colored edge for  $k$  odd. These cases reflect the following lemma (which can alternatively be implied from Theorem 15 (B)-(C)) via the correspondence  $i \leftrightarrow k - i$ , ( $i \in [k+1]$ ).

**Observation 11. (A)** Every 0-colored edge is represented via  $\Phi = F\alpha^0F^{-1}$ . **(B)** Every 1-colored edge is represented via the composition  $\Psi$  of  $\Phi$  (first) and root rotation (second).

By Theorem 4(ii), the number  $\xi$  of contiguous pairs of vertices of  $M_k$  in each  $C_i$  with a common  $k$ -germ happens in pairs. The first cases for which this  $\xi$  is null happens for  $k = 6$ , namely for the two reflection pairs  $(\rangle 012356 * * 4 * * * *), (\rangle 01235 * 46 * * * * * *)$  and  $(\rangle 01246 * 5 * * 3 * * *), (\rangle 0124 * 36 * 5 * * * * *)$  whose respective ordered trees are enantiomeric, i.e they are reflection via  $\Phi$  of each other. We say that these two cases are *enantiomeric*. In fact, two enantiomeric ordered trees in a case of an  $X(i)$  are distinguished by saying that the case is *enantiomeric*. For example,  $k = 4$  offers  $(\underline{1}, \underline{3})$  as the sole enantiomeric

pair in  $X(0)$ , and  $(\underline{2}, \underline{7})$ ,  $(\underline{4}, \underline{12})$ ,  $(\underline{11}, \underline{6})$  as all the enantiomorphic pairs in  $X(1)$ . Each enantiomorphic cycle  $C_i$  or each cycle  $C_i$  with  $\xi = 2$  has  $|C_i| = 2k(4k + 2)$ . If  $\xi = 2\zeta$  with  $\zeta > 1$ , then  $|C_i| = \frac{2k(4k+1)}{\zeta}$ . On account of these facts, we have the following:

**Observation 12.** *For each integer  $k > 1$ , there is a natural bijection  $\Lambda$  from the  $k$ -edge plane trees onto the cycles of  $W_{01}^k$ , as well as a partition  $\mathcal{P}_k$  of the  $k$ -germs (or the ordered trees they represent via  $F$ ), with each class of  $\mathcal{P}_k$  in natural correspondence either to a  $k$ -edge plane tree or to a pair of enantiomorphic  $k$ -edge plane trees disconnecting in  $W_{01}^k$  the forward (in  $L_k$ ) and reversed (in  $L_{k+1}$ ) readings of each vertex  $v$  of their associated cycles via  $\Lambda$ .*

## 12 Stepwise-Reversing View of Hamilton Cycles in $M_k$

For each cycle  $C_i$  of  $W_{01}^k$ , the ordered trees of its plane tree  $\mathcal{T}_i$  with leftmost subpath of length 1 from  $v_0$  to a vertex  $v_h$  determine 6-cycles touching  $C_i$  in two nonadjacent edges as follows: Let  $t_i < k$  be the number of degree 1 vertices of  $\mathcal{T}_i$ . Let  $\tau_i$  be the number of rotation symmetries of  $\mathcal{T}_i$ . Then, there are  $\frac{t_i}{\tau_i}$  classes mod  $n$  of pairs of vertices  $u, v$  at distance 5 in  $C_i$  with  $u \in L_{k+1}$  ahead of  $v \in L_k$  in  $X(i)$  and associated color  $h \in \{2, \dots, k\}$  such that: (i)  $u$  and  $v$  are adjacent via  $h$ ; (ii)  $u$  (resp.  $v$ ) has cyclic backward (resp. forward) reading  $\langle \dots * h0 * \dots \langle \dots * 0h * \dots \rangle$ ; (iii) the column in which the occurrences of  $h$  in (ii) happen at distance 5 looks between  $u$  and  $v$  (both included) as the transpose of  $(h, *, 0, 0, *, h)$ . Recall there are  $n$  such columns. In each case, the vertices  $u'$  and  $v'$  in  $C_i$  preceding respectively  $u$  and  $v$  in  $X_i$  are endvertices of a 3-path  $u'u''v''v'$  in  $M_k$  with the edge  $u''v''$  in a cycle  $C_j \neq C_i$  in  $W_{01}^k$ . The 6-cycle  $U_i^j = (uu'u''v''v'v)$  has as symmetric difference  $U_i^j \Delta (C_i \cup C_j)$  a cycle in  $M_k$  whose vertex set is  $V(C_i \cup C_j)$ . With  $u', u'', v'', v', v, u, u'$  shown vertically, Figure 5 illustrates  $U_i^j$ , twice each for  $k = 3, 4$ . That symmetric difference replaces respectively the edges  $u''v'', v'v$ ,  $uu'$  in  $C_i \cup C_j$  by  $u'u''$ ,  $v''v''$ ,  $vu$ . In the figure, vertically contiguous positions holding a common number  $g$  (meaning adjacency via color  $g$ ) are presented in red if  $g \in \{0, 1\}$ , e.g.  $u''v''$  with  $g = 1$ , in column say  $r_1$  exactly at the position where  $u$  and  $v$  differ, (however having common color  $h$  as in (i) above) and in orange, otherwise. The column  $r_2$  (resp  $r_3$ ) in each instance of Figure 4 containing color 1 in  $u'$  (resp. 0 in  $v'$ ) and a color  $c \in \{2, \dots, k\}$  in  $v'$  (resp. color  $d \in \{2, \dots, k\}$  in  $u'$ ) starts with  $1, *, c, c$ , (resp.  $d, d, *, 0$ ), where  $c, d \in \{2, \dots, k\}$ . Then,  $r_1, r_2, r_3$  are the only columns having changes in the binary version of  $U_i^j$ . All other columns have their first four entries alternating asterisks and colors. In the first disposition in item (ii) above, we have that: (ii')  $u''$  (resp.  $v''$ ) has cyclic backward (resp. forward) reading  $\langle \dots d10 * \dots \langle \dots * 1 * 0 \dots \rangle$ .

In the previous paragraph, “ahead” can be replaced by “behind”, yielding additional 6-cycles  $U_i^j$  by modifying adequately the accompanying text.

**Theorem 13.** [4, 2] *Let  $0 < k \in \mathbb{Z}$ . A Hamilton cycle in  $M_k$  is obtained by means of the symmetric differences of  $W_{01}^k$  with the members of a set of pairwise edge-disjoint 6-cycles  $U_i^j$ .*

*Proof.* Clearly, the statement holds for  $k = 1$ . Assume  $k > 1$ . Let  $\mathcal{D}$  be the digraph whose vertices are the cycles  $C_i$  of  $W_{01}^k$ , with an arc from  $C_i$  to  $C_j$ , for each 6-cycle  $U_i^j$ , where  $C_i, C_j \in V(\mathcal{D})$  with  $i \neq j$ . Since  $M_k$  is connected, then  $\mathcal{D}$  is connected. Moreover, the

```

>2 * 1 3 * * 0> ε (11)=3 ε X(0); >0 1 3 * 2 * *> ε (10)=2 ε X(1); >0 1 3 4 * * 2 * *> ε (010)= 2 ε X(1); >0 1 4 * 3 * 2 * *> ε (120)=10 ε X(2);
<* 2 * 3 1 0 *< ε (10)=2 ε X(1); <* * * 3 2 1 0< ε (00)=0 ε X(0); <* * * 4 3 2 1 0< ε (000)= 0 ε X(0); <* * * 3 * 4 2 1 0< ε (100)= 5 ε X(1);
>3 * 2 * 1 * 0> ε (12)=4 ε X(1); >0 2 3 * * 1 *> ε (01)= 1 ε X(0); >0 2 3 4 * * * 1 *> ε (001)= 1 ε X(0); >0 2 4 * 3 * * 1 *> ε (101)= 6 ε X(1);
<* 3 2 0 * 1 *< ε (01)= 1 ε X(0); <* 2 * 3 0 * 1< ε (12)=4 ε X(1); <* 2 * * 4 3 0 * 1< ε (012)= 4 ε X(1); <* 2 * 3 * 4 0 * 1< ε (123)=13 ε X(2);
>3 * * 0 2 * 1> ε (11)=3 ε X(0); >2 * 1 * 0 3 *> ε (12)=4 ε X(1); >2 * 1 4 * * 0 3 *> ε (122)=12 ε X(1); >3 * 2 * 1 * 0 4 *> ε (123)=13 ε X(2);
<* 3 1 * 2 0 *< ε (11)=3 ε X(0); <* 1 * 2 * 3 0< ε (12)=4 ε X(1); <* 1 * * 4 2 * 3 0< ε (112)= 9 ε X(1); <* 1 * 2 * 3 * 4 0< ε (123)=13 ε X(2);
>2 * 1 3 * * 0> ε (11)=3 ε X(0); >0 1 3 * 2 * *> ε (10)=2 ε X(1); >0 1 3 4 * * 2 * *> ε (010)= 2 ε X(1); >0 1 4 * 3 * 2 * *> ε (120)=10 ε X(2);

```

Figure 5: Examples of 6-cycles  $U_i^j$  for  $k = 4, 5$

outdegree and indegree of every  $C_i$  in  $\mathcal{D}$  is  $2n\frac{t_i}{\tau_i}$  (see items (ii) and (ii') above), in proportion with the length of  $C_i$ , a  $\frac{1}{n}$ -th of which is illustrated in each yellow box of Figure 4. Consider a spanning tree  $\mathcal{D}'$  of  $\mathcal{D}$ . Since all vertices of  $\mathcal{D}$  have outdegree  $> 0$ , there is a  $\mathcal{D}'$  in which the outdegree of each vertex is 1. This way, we avoid any pair of 6-cycles  $U_i^j$  with common  $C_i$  in which the associated distance-6 subpaths from  $u'$  to  $v$  in  $C_i$  do not have edges in common. For each  $a \in A(\mathcal{D}')$ , let  $\nabla(a)$  be its associated 6-cycle  $U_i^j$ . Then,  $\{\nabla(a); a \in A(\mathcal{D}')\}$  can be selected as a collection of edge-disjoint 6-cycles. By performing all symmetric differences  $\nabla(a)\Delta(C_i \cup C_j)$  corresponding to these 6-cycles, a Hamilton cycle is obtained.  $\square$

## 13 Alternate Viewpoint of Ordered Trees

To have the viewpoint of [2], replace  $v_0$  by  $v_k$  as root of the ordered trees. We start with examples. Figure 6 shows on its left-hand side the 14 ordered trees for  $k = 4$  encoded at the bottom of Table I. Each such tree  $T = T(\alpha)$  is headed on top by its  $k$ -germ  $\alpha$ , in which the entry  $i$  producing  $T$  via castling is in red. Such  $T$  has its vertices denoted on their left and its edges denoted on their right, with their notation  $v_i$  and  $e_j$  given in Section 11. Castling here is indicated in any particular tree  $T = T(\alpha) \neq T(00 \cdots 0)$  by distinguishing in red the largest subtree common with that of the parent tree of  $T$  (as in Theorem 2) whose castling reattachment produces  $T$ . This subtree corresponds with substring  $X$  in Theorem 3. In each case of such parent tree, the vertex in which the corresponding tree-surgery transformation leads to such a child tree  $T$  is additionally labeled (on its right) with the expression of its  $k$ -germ, in which the entry to be modified in the case is set in red color.

On the other hand, the 14 trees in the right-hand side of Figure 6 have their labels set by making the root to be  $v_k$  (instead of  $v_0$ ), then going downward to  $v_0$  (instead of  $v_k$ ) while gradually increasing (instead of decreasing) a unit in the subindex  $j$  of the denomination  $v_j$ , sibling by sibling from left to right at each level. The associated  $k$ -germ headers on this right-hand side of the figure correspond to the new root viewpoint. This determines a bijection  $\Theta$  established by correspondence between the old and the new header  $k$ -germs. In our example, it yields an involution formed by the pairs  $(001, 100)$ ,  $(011, 110)$ ,  $(120, 012)$  and  $(112, 121)$ , with fixed 000, 010, 101, 111, 122 and 123.

The function  $\Theta$  seen from the  $k$ -germ viewpoint, namely as the composition function  $F^{-1}\Theta F$ , behaves as follows. Let  $\alpha = a_{k-1}a_{k-2} \cdots a_2a_1$  be a  $k$ -germ and let  $a_i$  be the rightmost occurrence of its largest integer value. A substring  $\beta$  of  $\alpha$  is said to be an *atom* if it is either formed by a sole 0 or is a maximal strictly increasing substring of  $\alpha$  not starting with 0. For example, consider the 17-germ  $\alpha' = 0123223442310121$ . By enclosing the successive atoms between parentheses,  $\alpha'$  can be written as  $\alpha' = (0)123(2)(234)4(23)(1)(0)(12)(1)$ ,

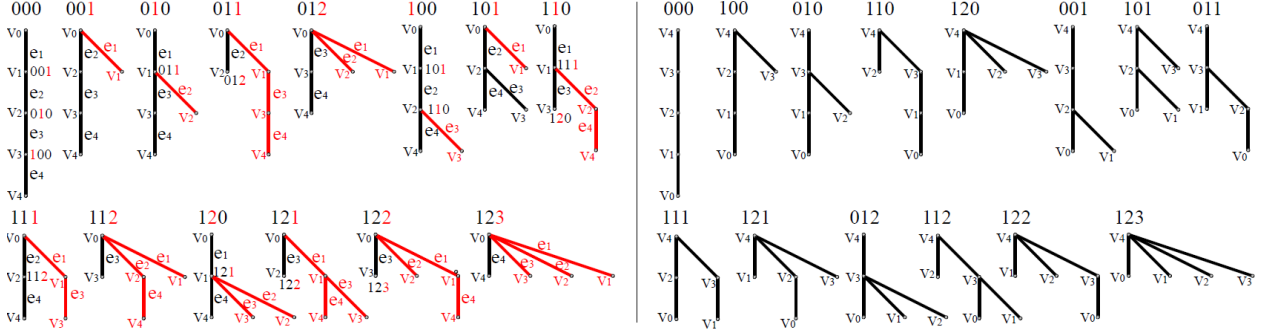


Figure 6: Generation of ordered trees for  $k = 4$

obtained by inserting in a *base string*  $\gamma' = 1 \cdots a_i = 1234$  all those atoms according to their order, where  $\gamma'$  appears partitioned into subsequent un-parenthesized atoms distributed and interspersed from left to right in  $\alpha'$  just once each as further to the right as possible. This atom-parenthesizing procedure works for every  $k$ -germ  $\alpha$  and determines a corresponding base string  $\gamma$ , like the  $\gamma'$  in our example.

**Theorem 14.** *Given a  $k$ -germ  $\alpha = a_{k-1}a_{k-2} \cdots a_2a_1$ , let  $a_i$  be the leftmost occurrence of its largest integer value. Then,  $\alpha$  is obtained from a base string  $\gamma = 1 \cdots a_i$  by inserting in  $\gamma$  all atoms of  $\alpha \setminus \gamma$  in their left-to-right order. Moreover,  $F^{-1}\Theta F(\alpha)$  is obtained by reversing the insertion of those atoms in  $\gamma$ , in right-to-left fashion. For both insertions,  $\gamma$  is partitioned into subsequent atoms distributed in  $\alpha$  and  $F^{-1}\Theta F(\alpha)$  as further to the right as possible.*

*Proof.*  $F^{-1}\Theta F(\alpha)$  is obtained by reversing the position of the parenthesized atoms, inserting them between the substrings of a partition of  $\gamma$  as the one above but for this reversing situation. In the above example of  $\alpha'$ , it is  $F^{-1}\Theta F(\alpha') = (1)(12)(0)(1)12(234)34(23)(2)(0)$ .  $\square$

## 14 Germ Structure of 1-Factorizations

TABLE VIII

$m$	$\alpha$	$F(\alpha)$	$F^3(\alpha)$	$F^2(\alpha)$	$F^1(\alpha)$	$F^0(\alpha)$	$\alpha^3$	$\alpha^2$	$\alpha^1$	$\alpha^0$
0	0	012 **	—	012 **	02 * 1*	1 2 ** 0	—	0	1	0
1	1	02 * 1*	—	1 * 02*	012 **	2 * 1 * 0	—	1	0	1
0	00	0123 ***	0123 ***	013 * 2 **	023 * 1 *	123 *** 0	00	10	01	00
1	01	023 ** 1 *	1 * 023 **	1 * 03 * 2 *	0123 ***	2 * 13 ** 0	01	12	00	11
2	10	013 * 2 **	02 * 20 **	0123 ***	03 * 2 * 1 *	13 * 2 ** 0	11	00	12	10
3	11	02 * 13 **	013 * 2 **	13 * 02 *	02 * 13 **	10 * 2 * 3	10	11	11	01
4	12	03 * 2 * 1 *	2 * 1 * 03 *	1 * 023 **	013 * 2 **	3 * 2 * 1 * 0	12	01	10	12

We present each  $c \in V(R_k)$  via the pair  $\delta(v) = \{v, \aleph_\pi(v)\} \in R_k$  ( $v \in L_k/\pi$ ) of Section 8 and via the  $k$ -germ  $\alpha$  for which  $\delta(v) = \langle F(\alpha) \rangle$ , and view  $R_k$  as the graph whose vertices

are the  $k$ -germs  $\alpha$ , with adjacency inherited from that of their  $\delta$ -notation via  $F^{-1}$  (i.e. uncastling). So,  $V(R_k)$  is presented as in the natural ( $k$ -germ) listing (see Section 2).

To start with, examples of such presentation are shown in Table VIII for  $k = 2$  and 3, where  $m$ ,  $\alpha = \alpha(m)$  and  $F(\alpha)$  are shown in the first three columns, for  $0 \leq m < C_k$ . The neighbors of  $F(\alpha)$  are presented in the central columns of the table as  $F^k(\alpha)$ ,  $F^{k-1}(\alpha)$ ,  $\dots$ ,  $F^0(\alpha)$  respectively for the edge colors  $k, k-1, \dots, 0$ , with notation given via the effect of function  $\aleph$ . The last columns yield the  $k$ -germs  $\alpha^k, \alpha^{k-1}, \dots, \alpha^0$  associated via  $F^{-1}$  respectively to the listed neighbors  $F^k(\alpha), F^{k-1}(\alpha), \dots, F^0(\alpha)$  of  $F(\alpha)$  in  $R_k$ .

TABLE IX

$m$	$\alpha$	$\alpha^4$	$\alpha^3$	$\alpha^2$	$\alpha^1$	$\alpha^0$	$m$	$\alpha$	$\alpha^4$	$\alpha^3$	$\alpha^2$	$\alpha^1$	$\alpha^0$
0	000	000	100	010	001	000	7	110	100	111	110	012	010
1	001	001	101	012	000	011	8	111	111	110	122	011	111
2	010	011	121	000	112	110	9	112	101	122	112	010	112
3	011	010	120	011	111	001	10	120	122	011	100	123	120
4	012	012	123	001	110	122	11	121	121	010	121	122	101
5	100	110	000	120	101	100	12	122	120	112	111	121	012
6	101	112	001	123	100	121	13	123	123	012	101	120	123
—	—	—	—	—	—	—	—	—	—	—	—	—	—
		3**	***	3**	*2*	***1			3**	***	3**	*2*	***1

For  $k = 4$  and 5, Tables IX and X have a similar respective natural enumeration adjacency disposition. We can generalize these tables directly to *Colored Adjacency Tables* denoted  $CAT(k)$ , for  $k > 1$ . This way, Theorem 15(A) below is obtained as indicated in the aggregated last row upending Tables IX and X citing the only non-asterisk entry, for each of  $i = k, k-2, \dots, 0$ , as a number  $j = (k-1), \dots, 1$  that leads to entry equality in both columns  $\alpha = a_{k-1} \cdots a_j \cdots a_1$  and  $\alpha^i = a_{k-1}^i \cdots a_j^i \cdots a_1^i$ , that is  $a_j = a_j^i$ . Other important properties are contained in the remaining items of Theorem 15, including (B), that the columns  $\alpha^0$  in all  $CAT(k)$ , ( $k > 1$ ), yield an (infinte) integer sequence.

TABLE X

$m$	$\alpha$	$\alpha^5$	$\alpha^4$	$\alpha^3$	$\alpha^2$	$\alpha^1$	$\alpha^0$	$m$	$\alpha$	$\alpha^5$	$\alpha^4$	$\alpha^3$	$\alpha^2$	$\alpha^1$	$\alpha^0$
0	0000	0000	1000	0100	0010	0001	0000	21	1110	1111	1100	1221	0110	1112	1110
1	0001	0001	1001	0101	0012	0000	0011	22	1111	1110	1111	1220	0122	1111	0111
2	0010	0011	1011	0121	0000	0112	0110	23	1112	1122	1101	1233	0112	1110	1222
3	0011	0010	1010	0120	0011	0111	0001	24	1120	1011	1222	1121	0100	1123	1120
4	0012	0012	1012	0123	0001	0110	0122	25	1121	1010	1221	1120	0121	1122	0101
5	0100	0110	1210	0000	1120	1101	1100	26	1122	1112	1220	1223	0111	1121	1122
6	0101	0112	1212	0001	1123	1100	1121	27	1123	1012	1233	1123	0101	1120	1223
7	0110	0100	1200	0111	1110	0012	0010	28	1200	1220	0110	1000	1230	1201	1200
8	0111	0111	1211	0110	1122	0011	1111	29	1201	1223	0112	1001	1234	1200	1231
9	0112	0101	1201	0122	1112	0010	0112	30	1210	1210	0100	1211	1220	1012	1011
10	0120	0122	1232	0011	1100	1223	1220	31	1211	1222	0111	1210	1233	1011	1221
11	0121	0121	1231	0010	1121	1222	1101	32	1212	1212	0101	1232	1223	1010	1212
12	0122	0120	1230	0112	1111	1221	0012	33	1220	1200	1122	1111	1210	0123	0120
13	0123	0123	1234	0012	1101	1220	1233	34	1221	1221	1121	1110	1232	0122	1211
14	1000	1100	0000	1200	1010	1001	1000	35	1222	1211	1120	1222	0121	1112	
15	1001	1101	0001	1201	1012	1000	1011	36	1223	1201	1223	1122	1212	0120	1123
16	1010	1121	0011	1231	1000	1212	1210	37	1230	1233	0122	1011	1200	1234	1230
17	1011	1120	0010	1230	1011	1211	1001	38	1231	1232	0121	1010	1231	1233	1201
18	1012	1123	0012	1234	1001	1210	1232	39	1232	1231	0120	1212	1221	1232	1012
19	1100	1000	1110	1100	0120	0101	0100	40	1233	1230	1123	1112	1211	1231	0123
20	1101	1001	1112	1101	0123	0100	0121	41	1234	1234	0123	1012	1201	1230	1234
—	—	—	—	—	—	—	—	—	—	—	—	—	—	—	—
		4***	****	4***	*3***	**2*	***1		4***	****	4***	*3***	**2*	***1	

**Theorem 15.** Let:  $k > 1$ ,  $j(\alpha^k) = k-1$  and  $j(\alpha^{i-1}) = i$ , ( $i = k-1, \dots, 1$ ). Then: (A) each column  $\alpha^{i-1}$  in  $CAT(k)$ , for  $i \in [k] \cup \{k+1\}$ , preserves the respective  $j(\alpha^{i-1})$ -th entry of  $\alpha$ ; (B) the columns  $\alpha^k$  of all  $CAT(k)$ 's for  $k > 1$  coincide into an RGS sequence and thus into an

integer sequence  $\mathcal{S}_0$ , the first  $C_k$  terms of which form an idempotent permutation for each  $k$ ; **(C)** the integer sequence  $\mathcal{S}_1$  given by concatenating the  $m$ -indexed intervals  $[0, 2), [2, 5), \dots, [C_{k-1}, C_k)$ , etc. in column  $\alpha^{k-1}$  of the corresponding tables  $\text{CAT}(2), \text{CAT}(3), \dots, \text{CAT}(k)$ , etc. allows to encode all columns  $\alpha^{k-1}$ 's; **(D)** for each  $k > 1$ , there is an idempotent permutation given in the  $m$ -indexed interval  $[0, C_k)$  of the column  $\alpha^{k-1}$  of  $\text{CAT}(k)$ ; such permutation equals the one given in the interval  $[0, C_k)$  of the column  $\alpha^{k-2}$  of  $\text{CAT}(k+1)$ .

*Proof.* (A) holds as a continuation of the observation made above with respect to the last aggregated row in Tables IX and X. Let  $\alpha$  be a  $k$ -germ. Then  $\alpha$  shares with  $\alpha^k$  (e.g. the leftmost column  $\alpha^i$  in Tables VIII to X, for  $0 \leq i \leq k$ ) all the entries to the left of the leftmost entry 1, which yields (B). Note that if  $k = 3$  then  $m = 2, 3, 4$  yield for  $\alpha^{k-1}$  the idempotent permutation  $(2, 0)(4, 1)$ , illustrating (C). (D) can be proved similarly.  $\square$

The sequences in Theorem 15 (B)-(C) start as follows, with intervals ended in “,”:

$$\begin{array}{r} \{0\} \cup \mathbb{Z}^+ = 0, 1; 2, 3; 4; 5, 6, 7, 8, 9, 10, 11, 12, 13; 14, 15, 16, \dots \\ \hline (B) = 0, 1; 3, 2; 4; 7, 9, 5, 8, 6, 12, 11, 10, 13; 19, 20, 25, \dots \\ (C) = 1, 0; 0, 3, 1; 0, 1, 8, 7, 12, 3, 2, 9, 4; 0, 1, 3, \dots \end{array}$$

*Remark 16.* With the notation of Section 13 and Theorem 14, for each of the involutions  $\alpha^i$  ( $0 < i < k$ ), it holds that  $\alpha^i \Theta = \Theta \alpha^{k-i}$ . This implies that

- (A) every  $k$ -colored edge represents an adjacency via  $\Phi' = F \alpha_k F^{-1}$  and
- (B) every  $(k-1)$ -colored edge represents an adjacency via  $\Psi' = F \Psi F^{-1}$ .

In addition, the reflection symmetry of  $\Phi'$  yields the sequence  $S_0$  cited in Theorem 15(B). A similar observation yields from  $\Psi'$  the sequence  $S_1$  cited in Theorem 15(C).

Given a  $k$ -germ  $\alpha = a_{k-1} \dots a_1$ , we want to express  $\alpha^k, \alpha^{k-1}, \dots, \alpha^0$  as functions of  $\alpha$ . Given a substring  $\alpha' = a_{k-j} \dots a_{k-i}$  of  $\alpha$  ( $0 < j \leq i < k$ ), let: **(a)** the *reverse string* off  $\alpha'$  be  $\psi(\alpha') = a_{k-i} \dots a_{k-j}$ ; **(b)** the *ascent* of  $\alpha'$  be **(i)** its maximal initial ascending substring, if  $a_{k-j} = 0$ , and **(ii)** its maximal initial non-descending substring with at most two equal nonzero terms, if  $a_{k-j} > 0$ . Then, the following remarks allow to express the  $k$ -germs  $\alpha^p = \beta = b_{k-1} \dots b_1$  via the colors  $p = k, k-1, \dots, 0$ , independently of  $F^{-1}$  and  $F$ .

*Remark 17.* Assume  $p = k$ . If  $a_{k-1} = 1$ , take  $0|\alpha$  instead of  $\alpha = a_{k-1} \dots a_1$ , with  $k-1$  instead of  $k$ , removing afterwards from the resulting  $\beta$  the added leftmost 0. Now, let  $\alpha_1 = a_{k-1} \dots a_{k-i_1}$  be the ascent of  $\alpha$ . Let  $B_1 = i_1 - 1$ , where  $i_1 = \|\alpha_1\|$  is the length of  $\alpha_1$ . It can be seen that  $\beta$  has ascent  $\beta_1 = b_{k-1} \dots b_{k-i_1}$  with  $\alpha_1 + \psi(\beta_1) = B_1 \dots B_1$ . If  $\alpha \neq \alpha_1$ , let  $\alpha_2$  be the ascent of  $\alpha \setminus \alpha_1$ . Then there is a  $\|\alpha_2\|$ -germ  $\beta_2$  with  $\alpha_2 + \psi(\beta_2) = B_2 \dots B_2$  and  $B_2 = \|\alpha_1\| + \|\alpha_2\| - 2$ . Inductively when feasible for  $j > 2$ , let  $\alpha_j$  be the ascent of  $\alpha \setminus (\alpha_1 \setminus \alpha_2) \dots \setminus \alpha_{j-1}$ . Then there is a  $\|\alpha_j\|$ -germ  $\beta_j$  with  $\alpha_j + \psi(\beta_j) = B_j \dots B_j$  and  $B_j = \|\alpha_{j-1}\| + \|\alpha_j\| - 2$ . This way,  $\beta = \beta_1 \setminus \beta_2 \dots \setminus \beta_j \dots$ .

*Remark 18.* Assume  $k > p > 0$ . By Theorem 15 (A), if  $p < k-1$ , then  $b_{p+1} = a_{p+1}$ ; in this case, let  $\alpha' = \alpha \setminus \{a_{k-1} \dots a_q\}$  with  $q = p+1$ . If  $p = k-1$ , let  $q = k$  and let  $\alpha' = \alpha$ . In both cases (either  $p < k-1$  or  $p = k-1$ ) let  $\alpha'_1 = a_{q-1} \dots a_{k-i_1}$  be the ascent of  $\alpha'$ . It can be seen that  $\beta' = \beta \setminus \{b_{k-1} \dots b_q\}$  has ascent  $\beta'_1 = b_{k-1} \dots b_{k-i_1}$  where  $\alpha'_1 + \psi(\beta'_1) = B'_1 \dots B'_1$  with  $B'_1 = i_1 + a_q$ . If  $\alpha' \neq \alpha'_1$  then let  $\alpha'_2$  be the ascent of  $\alpha' \setminus \alpha'_1$ . Then there is a  $\|\alpha'_2\|$ -germ  $\beta'_2$  where  $\alpha'_2 + \psi(\beta'_2) = B'_2 \dots B'_2$  with  $B'_2 = \|\alpha'_1\| + \|\alpha'_2\| - 2$ . Inductively when feasible for

$j > 2$ , let  $\alpha_j$  be the ascent of  $\alpha' \setminus (\alpha'_1|\alpha'_2|\cdots|\alpha'_{j-1})$ . Then there is a  $||\alpha'_j||$ -germ  $\beta'_j$  where  $\alpha'_j + \psi(\beta'_j) = B'_j \cdots B'_j$  with  $B'_j = ||\alpha'_{j-1}|| + ||\alpha'_j|| - 2$ . This way,  $\beta' = \beta'_1|\beta'_2|\cdots|\beta'_j|\cdots$ .

We process the left-hand side from position  $q$ . If  $p > 1$ , we set  $a_{a_q+2}\cdots a_q + \psi(b_{b_q+2}\cdots b_q)$  to equal a constant string  $B\cdots B$ , where  $a_{a_q+2}\cdots a_q$  is an ascent and  $a_{a_q+2} = b_{b_q+2}$ . Expressing all those numbers  $a_i, b_i$  as  $a_i^0, b_i^0$ , respectively, in order to keep an inductive approach, let  $a_q^1 = a_{a_q+2}$ . While feasible, let  $a_{q+1}^1 = a_{a_q+1}$ ,  $a_{q+2}^1 = a_{a_q}$  and so on. In this case, let  $b_q^1 = b_{b_q+2}$ ,  $b_{q+1}^1 = b_{b_q+1}$ ,  $b_{q+2}^1 = b_{b_q}$  and so on. Now,  $a_{a_q+2}^1\cdots a_q^1 + \psi(b_{b_q+2}^1\cdots b_q^1)$  equals a constant string, where  $a_{a_q+2}^1\cdots a_q^1$  is an ascent and  $a_{a_q+2}^1 = b_{b_q+2}^1$ . The continuation of this procedure produces a subsequent string  $a_q^2$  and so on, until what remains to reach the leftmost entry of  $\alpha$  is smaller than the needed space for the procedure itself to continue, in which case, a remaining initial ascent is shared by both  $\alpha$  and  $\beta$ . This allows to form the left-hand side of  $\alpha^p = \beta$  by concatenation.

## 15 Representations of $\delta(v)$

An independent way to obtain  $\delta(v)$  (not via its corresponding  $\alpha = \alpha(v)$ , which was the way we arrived to it in Section 8) is to take the representation corresponding to the lexical color 0 in  $\Gamma \subset \mathbb{R}^2$  (as in Figure 2, left), then rotating it around  $(0, 0)$  so that  $\partial$  becomes under the  $x$ -axis, and reflecting it on the  $x$ -axis, finally enlarging the grid with a scale factor of  $\sqrt{2}$ . This results in representations as in Figure 7 for  $k = 2, 3$ . In such representations, the lexical colors are set labeling the diagonal edges of the form  $(x, y)(x+1, y+1)$  and positioned in decreasing order from  $k$  to 0, from the top of the figure to its bottom and at each horizontal level from left to right. The diagonal edges of the form  $(x, y)(x-1, y-1)$  are set to carry an asterisk each. Figure 7 is indicated underneath each instance by the corresponding  $k$ -germ  $\alpha$  followed by its  $F(\alpha)$  and then by its (underlined) order of presentation via the castling. By recurring to all such piecewise-linear representations for a fixed  $k$ , we have a way to obtain all elements of  $R_k$  alternative to that given via Section 3, but without recurring to  $\alpha$ . This motivates the following definitions.

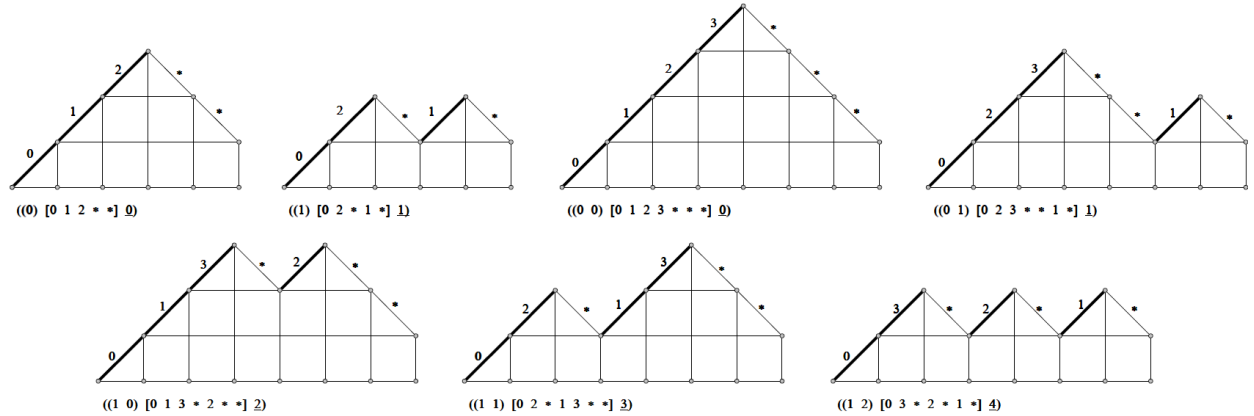


Figure 7: Representations of  $\delta(v)$  in  $R_2$  and  $R_3$

An oriented  $n$ -path (resp.  $n$ -cycle)  $G$  together with an assignment  $\eta : E(G) \rightarrow \{0, 1\}$  is

said to be a  $\mathbb{Z}_2$ -path (resp.  $Z_2$ -cycle) of weight  $= \sum_{e \in E(G)} \eta(e)$ . Each  $\mathbb{Z}_2$ -path  $P = u_0 u_1 \dots u_n$  in  $\mathbb{R}^2$  with  $u_i \in \mathbb{Z}^2$  for  $0 \leq i \leq n$  and  $|u_{i+1} - u_i| = \sqrt{2}$  for  $0 \leq i \leq n-1$  corresponds to its *piecewise-linear* (pl) representation, i.e., the plane path obtained as the union of the successive segments  $u_i u_{i+1} = (x_i, y_i), (x_i + d, y_i + d)$ , where  $d = 1$  (resp.  $d = -1$ ), if  $\eta(u_i u_{i+1})$  is 0 (resp. 1), starting at the origin  $u_0 = (0, 0)$ .

**Theorem 19.** *In each  $\mathbb{Z}_2$ -cycle graph  $C$  of weight  $k$  there is exactly one vertex  $u$  whose splitting into two vertices  $u'$  and  $u''$  and removal of the resulting arc  $u' u''$  transforms  $C$  into a  $\mathbb{Z}_2$ -path  $P_C$  of weight  $k$  and endvertices  $u', u''$  whose associated piecewise-linear representation touches the horizontal edge only at the origin, so that the lexical colors are assigned correctly, as in castling, to the vertices  $u$  with  $\eta(u) = 0$ .*

*Proof.* Clearly,  $C$  can be interpreted as a vertex of  $R_k$ . By the discussion above and the method exemplified in Figure 7, the vertex  $u$  in the statement must be selected as the starting vertex of the edge of  $C$  that is assigned the lexical color  $k$ . This leads to our claim.  $\square$

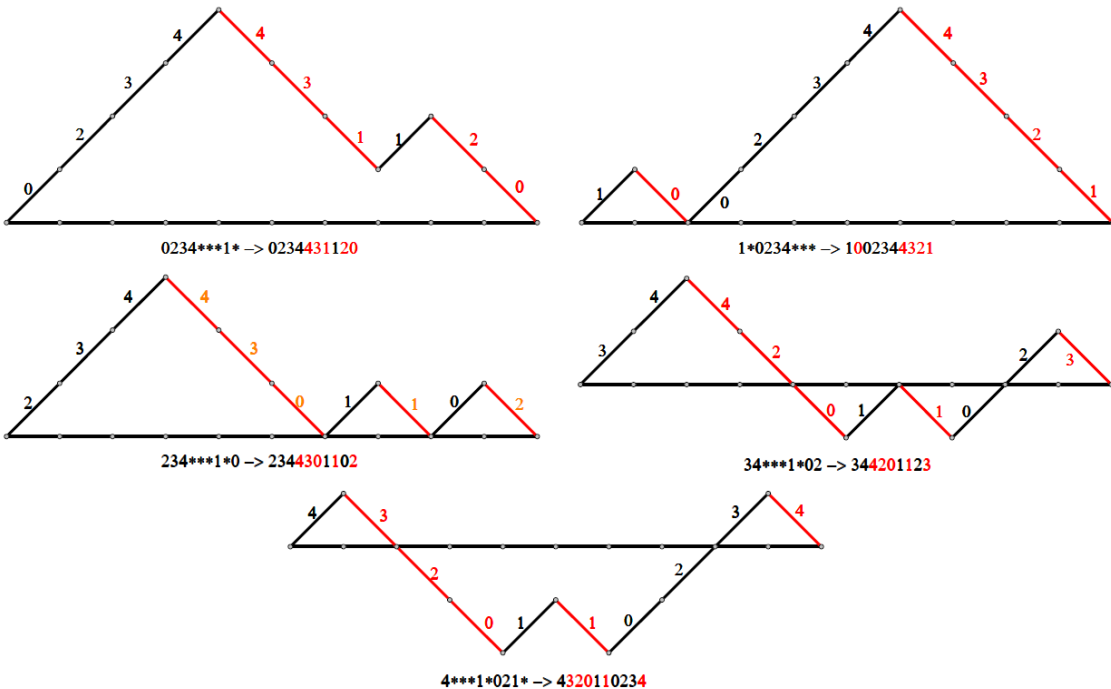


Figure 8: Examples of lexical-color adjacencies in  $R_4$

From now on, we omit the delimiting parentheses in expressing each  $v \in V(R_k)$ . The  $k$ -colored adjacency (Section 14) can be visualized by extending to the right each associated piecewise-linear representation (Figure 7) by a downward diagonal segment that touches the  $x$ -axis. This is exemplified in the upper left instance in Figure 8 for the vertex  $F(\alpha) = F(001) = 0234***1*$  of  $R_4$ , where red color is used to indicate the  $*$ -edges while taking into account the lexical-color criterion of Figure 7 backwards to set lexical colors from 0 to  $k$  (in red print now) to the  $*$ -edges always from top to bottom, and at each level from right to left. This yields a red-black path in the upper half of the cartesian plane with exactly two points

touching the  $x$ -axis, namely the initial and terminal points. Notice that this adjacency yields a notation for all the  $k$ -colored edges or loops of  $R_k$ .

This procedure yields also a notation for the other edges or loops in all  $R_k$ ; here, the corresponding piecewise-linear representations may not only touch the  $x$ -axis more than twice but traverse to the lower half of the plane; the only extra provisions are that the first (black) edge is  $(0, 0)(1, 1)$ , the last (red) edge is  $(n - 1, 1)(n, 0)$  and both these edges have a common color in  $[0, k]$ . Figure 8 illustrates all these adjacencies and the resulting notation for the edges departing from the selected vertex of  $R_k$ .

## 16 Catalan's Triangle

Given  $0 \leq m \in \mathbb{Z}$ , to determine  $\beta(m)$  or  $\alpha(m)$ , we use *Catalan's triangle*  $\Delta$ , i.e. a triangular arrangement of integers starting with the following successive rows  $\Delta_j$ , for  $j = 0, \dots, 8$ :

where reading is linear, as in [9] [A009766](#). The numbers  $\tau_i^j$  in  $\Delta_j$  ( $0 \leq j \in \mathbb{Z}$ ), given by  $\tau_i^j = (j+i)!(j-i+1)/(i!(j+1)!)$ , are characterized by the following properties:

1.  $\tau_0^j = 1$ , for every  $j \geq 0$ ;
2.  $\tau_1^j = j$  and  $\tau_j^j = \tau_{j-1}^j$ , for every  $j \geq 1$ ;
3.  $\tau_i^j = \tau_i^{j-1} + \tau_{i-1}^j$ , for every  $j \geq 2$  and  $i = 1, \dots, j-2$ ;
4.  $\sum_{i=0}^j \tau_i^j = \tau_j^{j+1} = \tau_{j+1}^{j+1} = C_j$ , for every  $j \geq 1$ .

The determination of  $k$ -germ  $\beta(m)$  proceeds as follows. Let  $x_0 = m$  and let  $y_0 = \tau_k^{k+1}$  be the largest member of the second diagonal of  $\Delta$  with  $y_0 \leq x_0$ . Let  $x_1 = x_0 - y_0$ . If  $x_1 > 0$ , then let  $Y_1 = \{\tau_{k-1}^j\}_{j=k}^{k+b_1}$  be the largest set of successive terms in the  $(k-1)$ -column of  $\Delta$  with  $y_1 = \sum Y_1 \leq x_1$ . Either  $Y_1 = \emptyset$ , in which case we take  $b_1 = -1$ , or not, in which case we take  $b_1 = |Y_1| - 1$ . Let  $x_2 = x_1 - y_1$ . If  $x_2 > 0$ , then let  $Y_2 = \{\tau_{k-2}^j\}_{j=k}^{k+b_2}$  be the largest set of successive terms in the  $(k-2)$ -column of  $\Delta$  with  $y_2 = \sum Y_2 \leq x_2$ . Either  $Y_2 = \emptyset$ , in which case we take  $b_2 = -1$ , or not, in which case we take  $b_2 = |Y_2| - 1$ . Iteratively, we arrive at a null  $x_k$ . Then  $\alpha(x_0) = a_{k-1}a_{k-2} \cdots a_1$ , where  $a_{k-1} = 1$ ,  $a_{k-2} = 1 + b_1$ ,  $\dots$ , and  $a_1 = 1 + b_k$ .

We note that  $\beta(m)$  is recovered from  $\alpha(m) = \alpha(x_0)$  by removing the zeros to the left of the leftmost 1 in  $\alpha(x_0)$ . Given an RGS  $\beta$  or associated  $k$ -germ  $\alpha$ , the considerations above can easily be played backwards to recover the corresponding integer  $x_0$ .

For example, if  $x_0 = 38$ , then  $y_0 = \tau_3^4 = 14$ ,  $x_1 = x_0 - y_0 = 38 - 14 = 24$ ,  $y_1 = \tau_2^3 + \tau_2^4 = 5 + 9 = 14$ ,  $x_2 = x_1 - y_1 = 24 - 14 = 10$ ,  $y_2 = \tau_1^2 + \tau_1^3 + \tau_1^4 = 2 + 3 + 4 = 9$ ,  $x_3 = x_2 - y_2 = 10 - 9 = 1$ ,  $y_3 = \tau_0^1 = 1$  and  $x_4 = x_3 - y_3 = 1 - 1 = 0$ , so that  $b_1 = 1$ ,  $b_2 = 2$ , and  $b_3 = 0$ , taking to  $a_4 = 1$ ,  $a_3 = 1 + b_1 = 2$ ,  $a_2 = 1 + b_2 = 3$  and  $a_1 = 1 + b_3 = 1$ , determining the 5-germ  $\alpha(38) = a_4a_3a_2a_1 = 1231$ . If  $x_0 = 20$ , then  $y_0 = \tau_3^4 = 14$ ,  $x_1 = x_0 - y_0 = 20 - 14 = 6$ ,  $y_1 = \tau_2^3 = 5$ ,  $x_2 = x_1 - y_1 = 1$ ,  $y_2 = 0$  is an empty sum (since its possible summand  $\tau_1^2 > 1 = x_2$ ),  $x_3 = x_2 - y_2 = 1$ ,  $y_3 = \tau_0^1 = 1$  and

$x_4 = x_3 - x_3 = 1 - 1 = 0$ , determining the 5-germ  $\alpha(20) = a_4a_3a_2a_1 = 1101$ . Moreover, if  $x_0 = 19$ , then  $y_0 = \tau_3^4 = 14$ ,  $x_1 = x_0 - y_0 = 19 - 14 = 5$ ,  $y_1 = \tau_2^3 = 5$ ,  $x_2 = x_1 - y_1 = 5 - 5 = 0$ , determining the 5-germ  $\beta(19) = a_4a_3a_2a_1 = 1100$ .

## References

- [1] J. Arndt, *Matters Computational: Ideas, Algorithms, Source Code*, Springer, 2011.
- [2] P. Gregor, T. Mütze and J. Nummenpalo, *A short proof of the middle levels theorem*, *Discrete Analysis*, 2018:8, 12pp.
- [3] H. A. Kierstead and W. T. Trotter, *Explicit matchings in the middle levels of the Boolean lattice*, *Order*, **5** (1988), 163–171.
- [4] T. Mütze, *Proof of the middle levels conjecture*, *Proc. LMS*, **112** (2016) 677–713.
- [5] T. Mütze, Torsten; Nummenpalo, Jerri Efficient computation of middle levels Gray codes. *ACM Trans. Algorithms* **14** (2018), no. 2, Art. 15, 29 pp.
- [6] T. Mütze, J. Nummenpalo and B. Walczak, *Sparse Kneser Graphs are Hamiltonian*, *STOC’18*, Proc. 50th Annual ACM SIGACT Symp. on Theory of Computing, 912–919, ACM, New York, 2018.
- [7] T. Mütze and J. Nummenpalo, *A Constant-Time Algorithm for Middle Levels Gray Codes*, *Algorithmica* **82** (2020), no. 5, 1239–1258.
- [8] I. Shields and C. Savage, *A Hamilton path heuristic with applications to the middle two levels problem*, *Congr. Num.*, **140** (1999), 161–178.
- [9] N. J. A. Sloane, The On-Line Encyclopedia of Integer Sequences, <http://oeis.org/>.
- [10] R. Stanley, *Enumerative Combinatorics*, Volume 2, (Cambridge Studies in Advanced Mathematics Book 62), Cambridge University Press, 1999.